# The Sloan Digital Sky Survey Monitor Telescope Pipeline

**D.L. Tucker**[1,*]**, S. Kent,**[1,2]**, M.W. Richmond,**[3]**, J. Annis,**[1]**, J.A. Smith,**[4,5,6]**, S.S. Allam,**[1,6]**, C.T. Rodgers,**[6]**, J.L. Stute,**[6]**, J.K. Adelman-McCarthy,**[1]**, J. Brinkmann,**[7]**, M. Doi,**[8]**, D. Finkbeiner,**[9,10,**]**, M. Fukugita,**[11]**, J. Goldston,**[10,12]**, B. Greenway,**[1]**, J.E. Gunn,**[10]**, J.S. Hendry,**[1]**, D.W. Hogg,**[13]**, S.-I. Ichikawa,**[14]**, Ž. Ivezić,**[10,15]**, G.R. Knapp,**[10]**, H. Lampeitl,**[1,16]**, B.C. Lee,**[1,17]**, H. Lin,**[1]**, T.A. McKay,**[18]**, A. Merrelli,**[19,20]**, J.A. Munn,**[21]**, E.H. Neilsen, Jr.,**[1]**, H.J. Newberg,**[22]**, G.T. Richards,**[10]**, D.J. Schlegel,**[10,17]**, C. Stoughton,**[1]**, A. Uomoto,**[23]**,** and **B. Yanny**[1]

[1] Fermi National Accelerator Laboratory, P.O. Box 500, Batavia, IL 60510, USA
[2] Department of Astronomy and Astrophysics, The University of Chicago, 5640 South Ellis Avenue, Chicago, IL 60637, USA
[3] Physics Department, Rochester Institute of Technology, 85 Lomb Memorial Drive, Rochester, NY 14623-5603, USA
[4] Deptartment of Physics & Astronomy, Austin Peay State University, P.O. Box 4608, Clarksville, TN 37044 USA
[5] Los Alamos National Laboratory, ISR-4, MS D448, Los Alamos, NM 87545-0000, USA
[6] Department of Physics and Astronomy, University of Wyoming, Laramie, WY 82071, USA
[7] Apache Point Observatory, P.O. Box 59, Sunspot, NM 88349, USA
[8] Institute of Astronomy, School of Science, University of Tokyo, Osawa 2-21-1, Mitaka, Tokyo 181-0015, Japan
[9] Harvard-Smithsonian Center for Astrophysics, 60 Garden Street, Cambridge, MA 02138, USA
[10] Princeton University Observatory, Peyton Hall, Princeton, NJ 08544, USA
[11] Institute for Cosmic Ray Research, University of Tokyo, 5-1-5 Kashiwa, Kashiwa City, Chiba 277-8582, Japan
[12] University of California at Berkeley, Departments of Physics and Astronomy, 601 Campbell Hall, Berkeley, CA 94720, USA
[13] Department of Physics, New York University, 4 Washington Place, New York, NY 10003, USA
[14] National Astronomical Observatory, 2-21-1 Osawa, Mitaka, Tokyo 181-8588, Japan
[15] Department of Astronomy, University of Washington, Box 351580, Seattle WA 98195-1580 USA
[16] Space Telescope Science Institute, 3700 San Martin Drive, Baltimore, MD 21218, USA
[17] Lawrence Berkeley National Laboratory, 1 Cyclotron Rd, Berkeley CA 94720-8160, USA
[18] Department of Physics, University of Michigan, 500 East University, Ann Arbor, MI 48109-1120, USA
[19] Department of Physics, Carnegie Mellon University, 5000 Forbes Avenue, Pittsburgh, PA 15232, USA
[20] Department of Astronomy, 105-24, California Institute of Technology, 1201 East California Boulevard, Pasadena, CA 91125, USA
[21] US Naval Observatory, Flagstaff Station, P.O. Box 1149, Flagstaff, AZ 86002, USA
[22] Department of Physics, Applied Physics, and Astronomy, Rensselaer Polytechnic Institute, 100 Eighth Street, Troy, NY 12180-3590, USA
[23] Observatories of the Carnegie Institution of Washington, 813 Santa Barbara Street, Pasadena, CA 91101, USA

The photometric calibration of the Sloan Digital Sky Survey (SDSS) is a multi-step process which involves data from three different telescopes: the 1.0-m telescope at the US Naval Observatory (USNO), Flagstaff Station, Arizona (which was used to establish the SDSS standard star network); the SDSS 0.5-m Photometric Telescope (PT) at the Apache Point Observatory (APO), New Mexico (which calculates nightly extinctions and calibrates secondary patch transfer fields); and the SDSS 2.5-m telescope at APO (which obtains the imaging data for the SDSS proper).

In this paper, we describe the Monitor Telescope Pipeline, MTPIPE, the software pipeline used in processing the data from the single-CCD telescopes used in the photometric calibration of the SDSS (i.e., the USNO 1.0-m and the PT). We also describe transformation equations that convert photometry on the USNO-1.0m $u'g'r'i'z'$ system to photometry the SDSS 2.5m $ugriz$ system and the results of various validation tests of the MTPIPE software. Further, we discuss the semi-automated PT factory, which runs MTPIPE in the day-to-day standard SDSS operations at Fermilab. Finally, we discuss the use of MTPIPE in current SDSS-related projects, including the Southern $u'g'r'i'z'$ Standard Star project, the $u'g'r'i'z'$ Open Star Clusters project, and the SDSS extension (SDSS-II).

# 1 Introduction

The Sloan Digital Sky Survey (SDSS; York et al. 2000; Stoughton et al. 2002a; Abazajian et al. 2003, 2004, 2005; Adelman-McCarthy et al. 2006) is a modern, CCD-based optical imaging and spectroscopic survey of the Northern Galactic Cap. Both imaging and spectroscopy are performed using a 2.5m f/5 Ritchey-Chrétien telescope (Gunn et al. 2006). The imaging camera (Gunn et al. 1998) contains an imaging array of thirty $2048 \times 2048$ SITe CCDs and scans the sky in drift scan mode along great circles in five different filters ($ugriz$). A complete scan from the western to the eastern borders of the survey area is called a *strip*. Since there are gaps within the CCD mosaic, it requires two strips, offset by 93% of a CCD width, to fill in a complete rectangular area (which is called *stripe*). The imaging portion of the SDSS has a depth of $r = 22.2$ (95% detection repeatablity for point sources; Ivezić et al. 2004). Followup spectrosopy is performed for a variety of targetted galaxies (Eisenstein et al. 2001; Strauss et al. 2002), quasars (Richards et al. 2002), and stars via a pair of 320-fiber multiobject spectrographs.

The SDSS imaging covers several thousand square degrees of sky, and over this region the SDSS photometric calibrations achieve an accuracy of $\approx$0.02 mag (2%) rms in $g$, $r$, and $i$ and $\approx$0.03 mag (3%) in $u$ and $z$ (Ivezić et al. 2004; Adelman-McCarthy et al. 2006). The photometric calibration of the SDSS 2.5m imaging data is a multi-step process which involves the data from three different telescopes and three different data processing pipelines. The telescopes in question are:

1. the US Naval Observatory (USNO) 1.0-m telescope at Flagstaff Station, Arizona, which was used to set up a network of 158 primary standard stars for the $u'g'r'i'z'$ photometric system in the magnitude range $9 \lesssim r' \lesssim 14$ (Fig. 1; Fukugita et al. 1996; Smith et al. 2002);
2. the 0.5-m Photometric Telescope (PT) at Apache Point Observatory (APO), New Mexico, which observes a set of $u'g'r'i'z'$ primaries over a range of airmasses to determine the photometric solution for the night (zeropoints & extinctions), and calibrates stars down to $r' \approx 18$ in transfer fields — or secondary patches — that are placed throughout the SDSS survey area (Fig. 2); and
3. the SDSS 2.5-m telescope itself (Gunn et al. 2006), also located at APO, whose imaging camera (Gunn et al. 1998) scans over the secondary patches (Fig. 2) during normal course of operations. Note that the imaging camera saturates under normal operating conditions at $r \approx 14$, necessitating the use of faint stars in the secondary patches (rather than observing the primary standards directly). The secondary patches, which are $40' \times 40'$ in size, are grouped in sets of four, so that each group spans

the full 2.5° width of a survey stripe, and each group is spaced at roughly 15° (1 hour) intervals along a survey stripe. [The positions of patches along a stripe have been optimized to avoid bright ($V \lesssim 8$) stars; hence the slight variability in the spacings between patch groups and between patches within patch groups.] To calibrate the 2.5m imaging camera photometry, atmospheric extinction measurements are taken from PT observations for the night, and photometric zeropoints are obtained by matching stars in the imaging camera data with those from the secondary patches. This method of calibration permits the 2.5m telescope to spend its time more efficiently, in that the onus of obtaining nightly extinction measurements and of calibrating primary and secondary standard stars is shifted to other, smaller telescopes.

The three software pipelines are:

1. the Monitor Telescope Pipeline (`MTPIPE`)[1], which was used to process the USNO-1.0m data for setting up the $u'g'r'i'z'$ primary standard star network (Smith et al. 2002), and which is currently used to process the PT data for determining the atmospheric extinctions at APO each night and for calibrating the secondary patch fields to the SDSS $ugriz$ system;
2. the Photometric Pipeline (`PHOTO`; Lupton et al. 2001; Lupton 2006), which processes the 2.5m imaging camera data, yielding among its many outputs accurate astrometry (Pier et al. 2003) and $ugriz$ instrumental photometry (counts); and
3. the (New) Final Calibrations Pipeline (`NFCALIB`; § 4.5.3. of Stoughton et al. 2002a), which matches the stars in the PT secondary transfer fields with the 2.5m imaging camera photometry, calculates the resulting photometric zeropoints, and applies them to the 2.5m instrumental magnitudes. (To deal with 2.5m imaging scans that are observed over a range of airmasses, `NFCALIB` also makes use of the first-order atmospheric extinction coefficients measured by the PT on the same night as a given imaging scan. Since most 2.5m imaging scans only cover a small range in airmass, this is typically a small effect.)

These pipelines were written with the expressed purpose of meeting the image processing and calibration needs of the SDSS, and are in no way meant to supplant the many excellent general-purpose astronomical image processing and analysis packages like IRAF[2] (Tody 1986, 1993), MIDAS[3] (Warmels 1985; Grosbøl 1989), Gypsy[4] (Shostek & Allen 1980; Allen et al. 1992; van der Hulst et al. 1992), SExtractor (Bertin & Arnouts 1996), DAOPHOT (Stetson 1987),

⋆ Corresponding author: e-mail: dtucker@fnal.gov

⋆⋆ Hubble Fellow

---

[1] The Monitor Telescope Pipeline is named after the original SDSS 0.6m calibration telescope at APO, called the Monitor Telescope (or MT), which was de-commissioned in Summer 1998 and replaced by the PT, which was commissioned in Spring 1999. Overlapping this time frame, the USNO-1.0m telescope was used to set up the $u'g'r'i'z'$ standard star network, a task originally planned for the old MT.
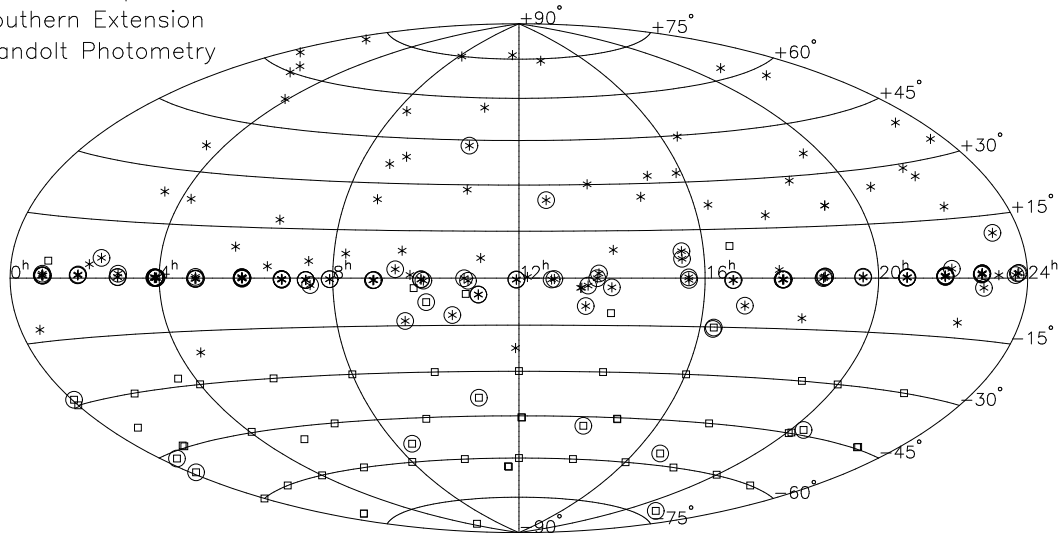
[2] `iraf.noao.edu`

[3] `http://www.eso.org/projects/esomidas/`

[4] `http://www.astro.rug.nl/~gipsy/`

**Fig. 1** Locations of the 158 Smith et al. (2002) primary standards (asterisks) and the 64 fields of the southern extension to the primary standard star network (unfilled squares; see § 5). Circled symbols indicate $u'g'r'i'z'$ standard stars or fields for which there is currently Landolt $UBVR_cI_c$ photometry (Landolt 1973, 1983, 1992) or for which Landolt is currently obtaining $UBVR_cI_c$ photometry (Landolt, in prep.).
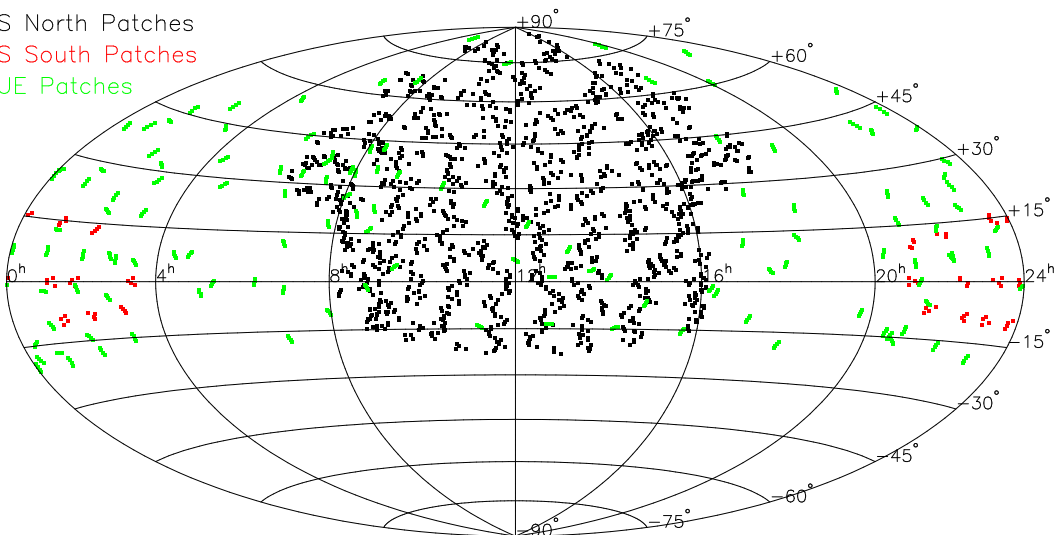


**Fig. 2** Locations of the SDSS secondary patches in equatorial coordinates (Aitoff projection): *(black)* Northern SDSS patches, *(red)* Southern SDSS patches, and *(green)* SEGUE patches. (SEGUE is part of the Sloan extension, or SDSS-II, and is discussed in § 5.)

and DoPHOT (Schechter et al. 1993), to name but a few. Thus, the SDSS imaging and photometric calibration pipelines have more in common with such special-purpose software packages as the ESO Imaging Survey pipeline (Nonino et al. 1999), the INT Wide Field Camera pipeline (Irwin & Lewis 2001), the VLT Survey Telescope pipeline (Grado et al. 2004), and the Liverpool Telescope Gamma Ray Burst pipeline (Guidorzi et al. 2006).

The topic of the current paper is `MTPIPE`. In the following sections, we will discuss in turn `MTPIPE`'s component packages (§ 2), validation tests of the `MTPIPE` software (§ 3), the `MTPIPE`-based semi-automated PT data processing factory (§ 4), and other SDSS-related projects using `MTPIPE` (§ 5); in § 6 we comment on future plans for `MTPIPE`.

In closing, we note that, although the SDSS magnitudes and colors are shown without primes ($ugriz$), the magnitudes of the primary standard stars are shown with primes ($u'g'r'i'z'$). This is no accident. The primed system is defined in the natural system of the USNO-1.0m, its CCD, and its set of SDSS filters. The SDSS magnitudes, however, are defined in the natural system of the SDSS 2.5m imag-
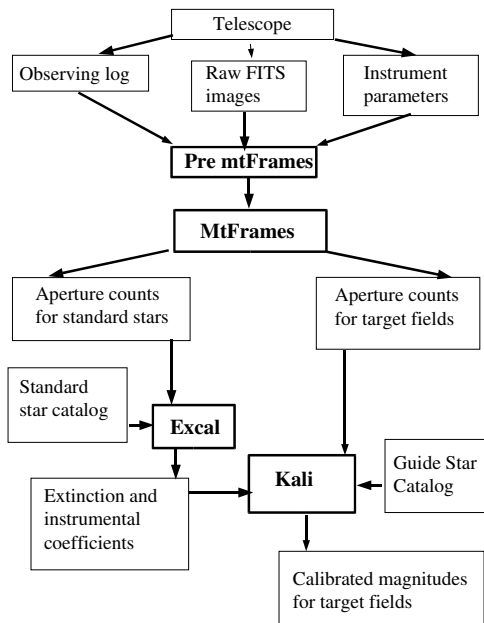
**Fig. 3** A flowchart of `MTPIPE`.

ing camera and its SDSS filters. These two systems are very similar and the coefficients of the transformation equations are quite small. We will describe the differences in these two systems and provide transformation equations in § 2.

## 2 The `MTPIPE` packages

`MTPIPE` is a suite of code written in a combination of the Tcl and C programming languages and based upon the SDSS `DERVISH+ASTROTOOLS` (Stoughton 1995; Sergey et al. 1996) software environment. The current version of `MTPIPE` is `v8.3`, although changes since `v8.0` have been mostly cosmetic and have generally dealt with the smooth running of the PT Factory (§ 4). `MTPIPE` includes four main packages used in normal reductions: `preMtFrames`, `mtFrames`, `excal`, and `kali`, and they are run in that order (Fig. 3).

### 2.1 `preMtFrames`

The first package, `preMtFrames`, is basically a "pre-burner": it creates the directory structure for the reduction of a night's data, including various parameter files needed as input for the other three packages, and it runs quality assurance tests on the raw data. Furthermore, it verifies information in the electronically generated observing log (which is based upon the information within the FITS image headers), identifies the type of each image (e.g., bias frame, dome flat, twilight flat, primary standard field, survey secondary patch field, or specially targetted manual fields), matches the frame identifier to a list of approved standard fields, verifies that a full set of frames ($u'g'r'i'z'$) are present for each target sequence, and creates histograms for each of the bias and flat field frames.

As an example, plotted in Figure 4 are histograms showing the distribution of pixel values for each of the bias frames observed by the PT on MJD 53501.[5] Note that the PT CCD uses two-amplifier readout, as evidenced by the strongly bimodal distribution of pixel values for these bias frames.

Note that `MTPIPE` does not use the values of image FITS header keywords directly, but makes use of an ASCII observing log (called the mdReport file) containing the relevant information (e.g., RA, DEC, time of observation, exposure time, filter, ...) for each image. This information is usually based upon image FITS header keyword values, but can also be user-generated. The use of the mdReport file simplifies the process of editing this information by humans when the need arises.
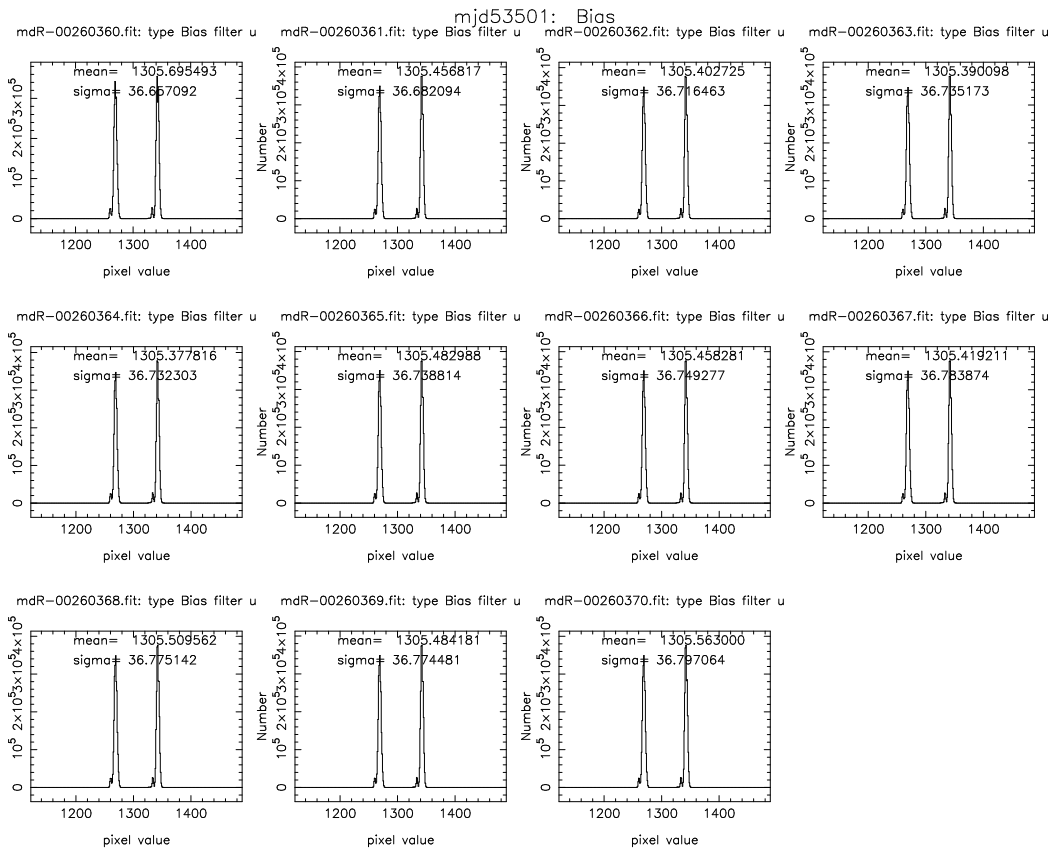
### 2.2 `mtFrames`

The next package, `mtFrames`, is the primary image processing portion of the software, and is capable of processing data from CCDs with 1-, 2-, or 4-amplifier readout electronics.

The first part of `mtFrames` creates master bias frames, flat field frames, and fringe frames. The master biases are created by median filtering a set raw bias frames. During general operations with the PT, typically ten raw bias frames are obtained per night.

Once the master bias is created, master dome flats for each filter are made; this is done by subtracting the master bias from each raw dome flat frame, removing any residual median offset from the overscan regions, trimming off the overscan region, applying any linearity corrections, and median filtering the thus-processed individual dome flats for a given filter. For the PT, typically five raw dome flats are obtained for each of the five filters ($u'g'r'i'z'$) every afternoon of scheduled observing. The same processing steps are employed to create master twilight flats from the raw twilight flat frames. For the PT, raw twilights are obtained mostly in $u'$, since we find that dome flats sufficiently flatten the PT $g'r'i'z'$ frames, whereas only twilight flats are capable of adequately flattening the PT $u'$ frames. Typically 5-10 raw twilights (mostly in $u'$) are obtained each evening twilight in which the skies are reasonably clear.

Master fringe frames are needed to remove the additive effects of internal CCD illumination patterns seen in the $i'$ and $z'$ filters. To create master $i'$ and $z'$ fringe frames, `mtFrames` seeks out all the secondary patches observed during a night. These secondary patches are useful for creating master fringe frames because they are relatively deep (i.e., have relatively long exposure times), and because they are of relatively uncrowded star fields containing few if any bright (highly saturated) stars, and because a given secondary patch is typically not repeat-targetted during a given night. If there are a sufficient number of secondary patches observed on that night (for the PT, the default minimum is

---

[5] MJD is the Modified Julian Date, defined by the relation MJD ≡ JD − 2,400,000.5, where JD is the Julian Date.

mjd53501: Bias

mdR−00260360.fit: type Bias filter u    mdR−00260361.fit: type Bias filter u    mdR−00260362.fit: type Bias filter u    mdR−00260363.fit: type Bias filter u

mean= 1305.695493    mean= 1305.456817    mean= 1305.402725    mean= 1305.390098
sigma= 36.657092     sigma= 36.682094     sigma= 36.716463     sigma= 36.735173

mdR−00260364.fit: type Bias filter u    mdR−00260365.fit: type Bias filter u    mdR−00260366.fit: type Bias filter u    mdR−00260367.fit: type Bias filter u

mean= 1305.377816    mean= 1305.482988    mean= 1305.458281    mean= 1305.419211
sigma= 36.732303     sigma= 36.738814     sigma= 36.749277     sigma= 36.733874

mdR−00260368.fit: type Bias filter u    mdR−00260369.fit: type Bias filter u    mdR−00260370.fit: type Bias filter u

mean= 1305.509562    mean= 1305.484181    mean= 1305.563000
sigma= 36.775142     sigma= 36.774481     sigma= 36.797064

**Fig. 4**    Histograms of pixel values for each of the raw PT bias frames taken on MJD 53501. Note that the PT's CCD has 2-amplifier readout electronics; hence, the bimodality of the distributions.

7), master fringe frames will be created for the $i'$ and $z'$ filters. The $i'$ and $z'$ frames for the secondary patches are fully processed up through flatfielding — they are bias-subtracted using the master bias, their residual overscan offset is subtracted, their overscan is trimmed, they are linearity corrected, and they are flatfielded with the appropriate master flat frame. After this processing, the secondary patch frames for a given filter are scaled to a default median background sky and median filtered. This final median-filtered image is the fringe frame for that filter.

Note that, in the above description of creating master biases, flats, and fringes, we only make mention of data obtained over a single afternoon+night. Why not use the data obtained over a full week or month or more to beat down statistics? Actually, it is possible to do this with `mtFrames`, if one collects all the data from a multiple-night run into a single directory and manipulates the ASCII observing log file appropriately; this process is currently not automated, and hence requires a certain level of human interaction. With general PT operations for the SDSS, however, the guiding principle is that of considering each night as a self-contained experiment. Often, obtaining photometric calibration data for the SDSS is time critical, and it is ill-advised to wait until the end of a dark run to obtain (hopefully) all the nec-

essary bias, flat, and fringe frames. That said, those nights when it is impossible to obtain a sufficient set of biases, flats, or (which is more often the case) secondary patches for fringe frames, the necessary master frames are copied from another night's processed data. This is permissible since the PT's biases and flats are stable over the course of a typical 3-week observing run — significant discontinuous changes in these calibration frames are, however, often noticeable from one observing run to the next — and the PT $i'$ and $z'$ band fringe patterns — being an artifact of physical variations in the thickness of the CCD itself — are stable over even longer periods.

The second part of `mtFrames` applies these master biases, flats, and fringe frames to the target frames — i.e., to the frames of fields containing primary standard stars, of secondary patch fields, and of any manually targetted fields of interest. The standard processing steps apply: for a target frame in a given filter, the master bias is subtracted, any residual median offset from the overscan regions is subtracted, the frame is trimmed of the overscan regions, a linearity correction is applied, and the appropriate master flat frame is used; if the target frame is in the $i'$ or $z'$ filter, a fringe frame is subtracted and the median sky value of pre-defringed frame is added back to all the pixels.
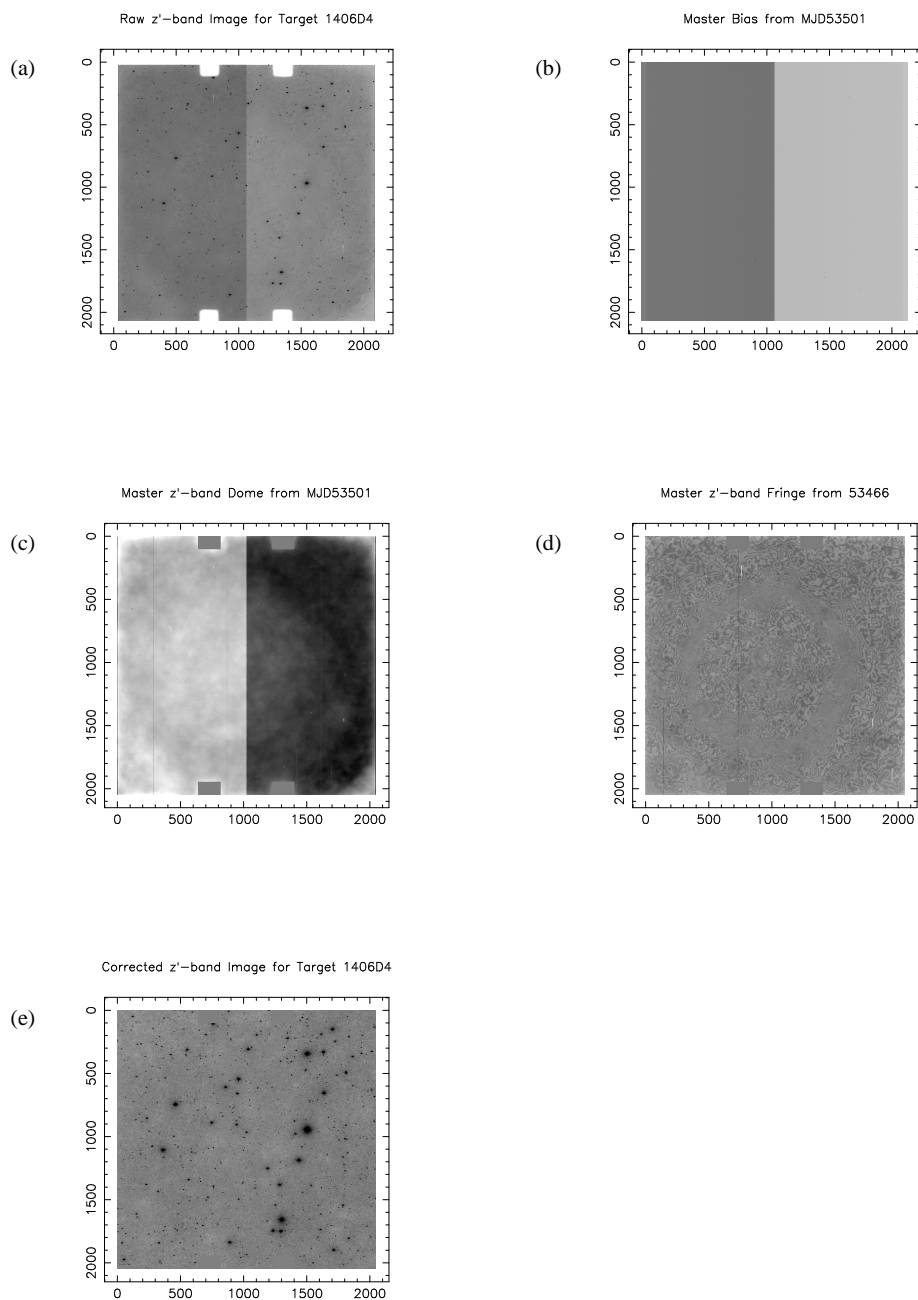
**Fig. 5** The image processing steps, using PT data from MJD 53501 as an example: (a) the raw $z'$-band image of the secondary patch 1406D4, (b) the master bias frame from MJD 53501, (c) the master $z'$-band dome flat from MJD 53501, (d) master $z'$-band fringe frame from MJD 53466 (used for processing the PT data from MJD 53501), (e) the bias-subtracted, trimmed, flat-fielded, and fringe-corrected $z'$-band image of the secondary patch 1406D4. The (linear) stretch used in these images is from 90% to 110% of the given image's median pixel value.

Once a target frame is fully processed, objects are detected as peaks $n\sigma$ above the sky background, where $\sigma$ is the rms scatter in the sky background, and aperture photometry is performed (for the general PT operations, $n = 10$). For the aperture photometry, one of two apertures may be used. The larger aperture is used for fields containing standard stars and for bright stars in secondary patches and manual target-of-opportunity fields. The smaller aperture is used for faint stars in the secondary patches and manual fields; an aperture correction is applied to convert the small aperture counts into a measure of the large aperture counts for these faint stars. The actual sizes of these apertures are parameters that can be adjusted. For example, when setting up the original standard star network (Smith et al. 2002), the
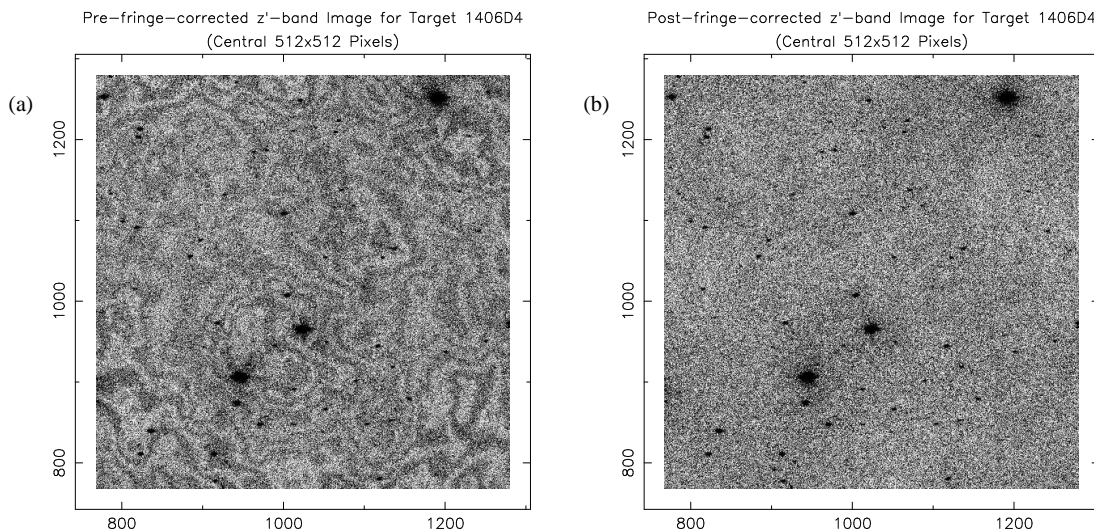
**Fig. 6** An example of de-fringing a PT $z'$-band image: (a) the central $512 \times 512$ pixels of the bias-subtracted, trimmed, flat-fielded, but not fringe-corrected $z'$-band image of the field featured in Figure 5; (b) the same as (a), but after fringe-correction. The (linear) stretch in these two images is the same (from 95% to 105% of the median pixel value of (a)). The typical trough-to-peak amplitudes of the fringes in (a) is $\approx 2\%$.

primary standard stars were extracted using a 24-arcsec diameter aperture. This size was selected to avoid problems associated with defocussing the brightest stars, required for some of the USNO observations.

Typically a given field is observed in multiple filters before moving on to the next field, yielding a sequence of target frames for that field, one for each filter. In general PT operations, each target field is observed in all five filters ($u'g'r'i'z'$) before moving on to the next target field. Once `mtFrames` has performed aperture photometry on all the frames for a given $u'g'r'i'z'$ sequence, objects detected in each filter are matched (by default, they are matched to the detected objects in the $r'$ filter) and the merged object list is written to disk as a FITS binary table file. For the PT, which has a known radial distortion, a distortion correction is applied at this stage to the aperture photometry.

As an example of the processing steps in `mtFrames`, we continue our examination of the PT data from MJD 53501. In Figure 5, we see a raw $z'$ image for one of the secondary patches observed that night (Fig. 5a), the master bias for that night (Fig. 5b), the master $z'$-band dome flat for that night, (Fig. 5c), the master $z'$-band fringe frame for that night (actually taken from MJD 53466, due to an insufficient number of secondary patches observed on MJD 53501; Fig. 5d), and the final, bias-subtracted, flat-fielded, de-fringed $z'$ corrected frame for that secondary patch (Fig. 5e). In Figure 6, we zoom in on the central quarter of the pre- and post-fringe-corrected frame to show the effects of de-fringing.

Finally, `mtFrames` outputs quality assurance plots for the night processed. Two examples are shown in Figure 7: Figure 7a and b show, respectively, the sky brightness (in ADU counts per pixel) vs. time and the mean FWHM per

**Table 1** PT Color Indices (`excal` & `kali`)

| filter | color index |
|--------|-------------|
|        | $(x - y)_\mathrm{o}$ |
| $u'$ | $(u' - g')_\mathrm{o}$ |
| $g'$ | $(g' - r')_\mathrm{o}$ |
| $r'$ | $(r' - i')_\mathrm{o}$ |
| $i'$ | $(r' - i')_\mathrm{o}$ |
| $z'$ | $(i' - z')_\mathrm{o}$ |

**Table 2** PT Color Zeropoints (`excal` & `kali`)

| color zeropoint | value |
|-----------------|-------|
| $(u' - g')_\mathrm{o,zp}$ | 1.39 |
| $(g' - r')_\mathrm{o,zp}$ | 0.53 |
| $(r' - i')_\mathrm{o,zp}$ | 0.21 |
| $(i' - z')_\mathrm{o,zp}$ | 0.09 |

image vs. time for PT data obtained on the night of MJD 53501.

### 2.3 excal

The third package, `excal`, takes the output of `mtFrames` for the $u'g'r'i'z'$ standard star fields, identifies the individual standard stars within these fields, and — using the instrumental magnitudes for these stars as input — invokes a least squares routine to calculate the photometric zeropoint and the atmospheric extinction in each filter passband. Since the overall system response in each filter (which is measured by the photometric zeropoints) is unlikely to change significantly over the course of single night, a single photometric zeropoint is calculated for a night. On the other hand, changes in the atmospheric transparency in each filter

## Normalized sky value in MT images for run 53501
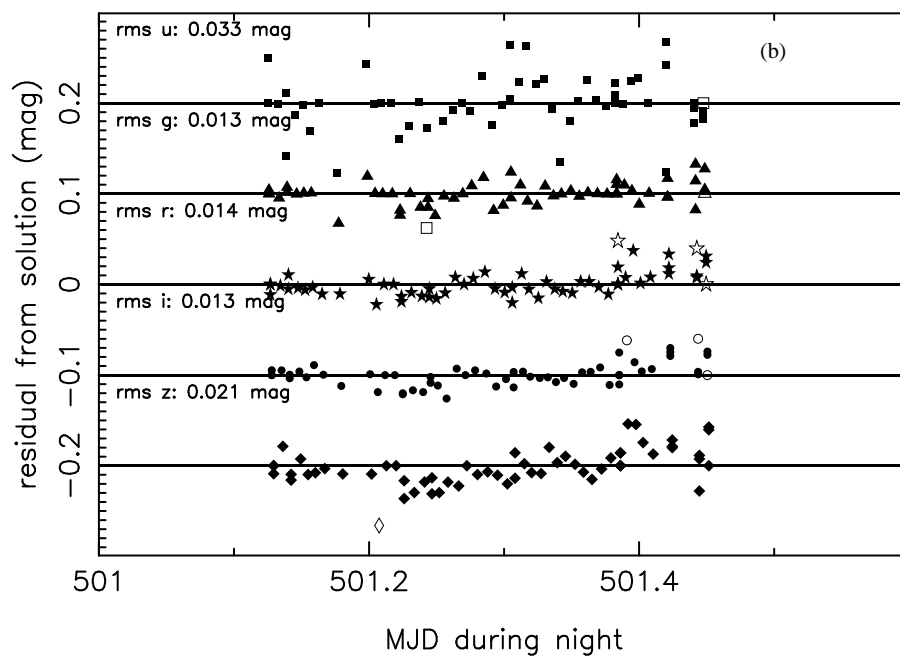


## FWHM (pixels) in MT images for run 53501
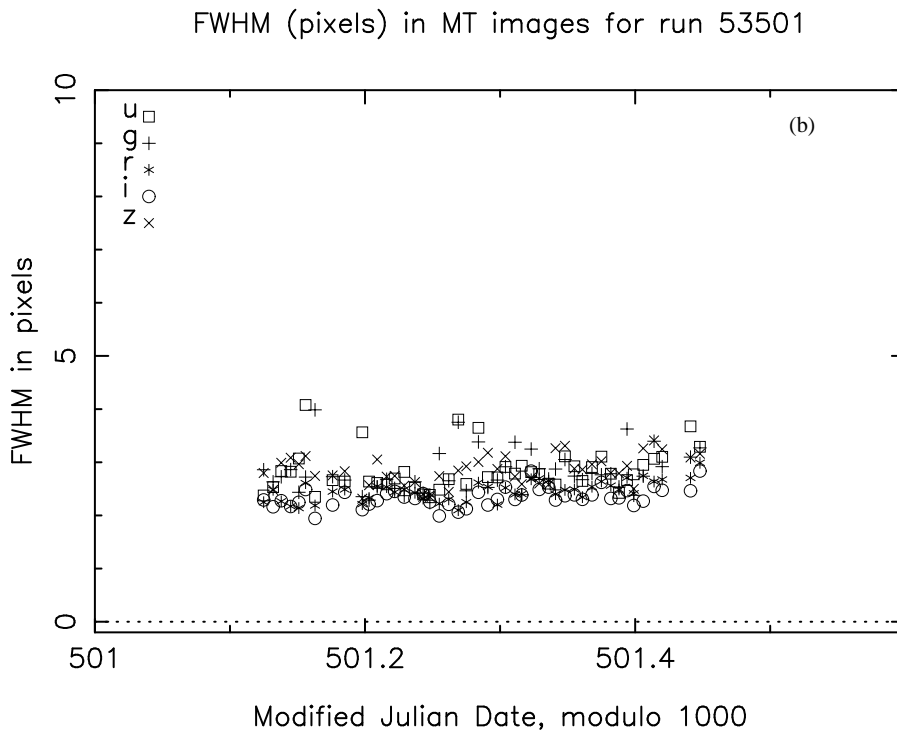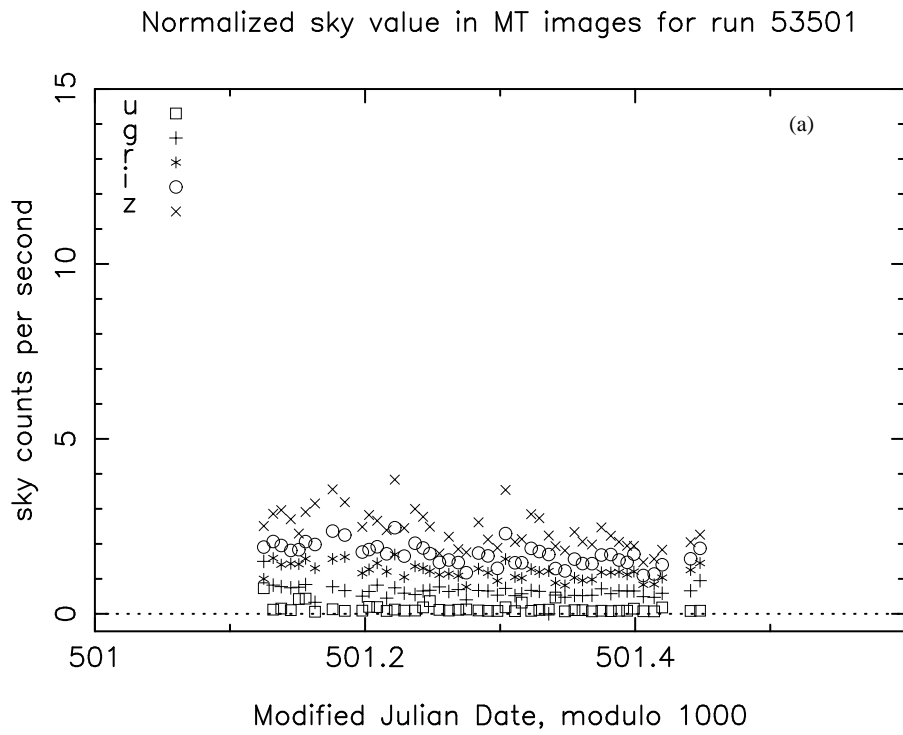


**Fig. 7** A sampling of the quality assurance plots output by `mtFrames` for the PT data taken on the night of MJD 53501: (a) Sky counts (in ADU/pixel) vs. time in each of the five passbands; (b) Mean image FWHM (in pixels) vs. time in each of the five passbands. (Note that the scale of the PT's CCD is $1.15''$/pixel.)
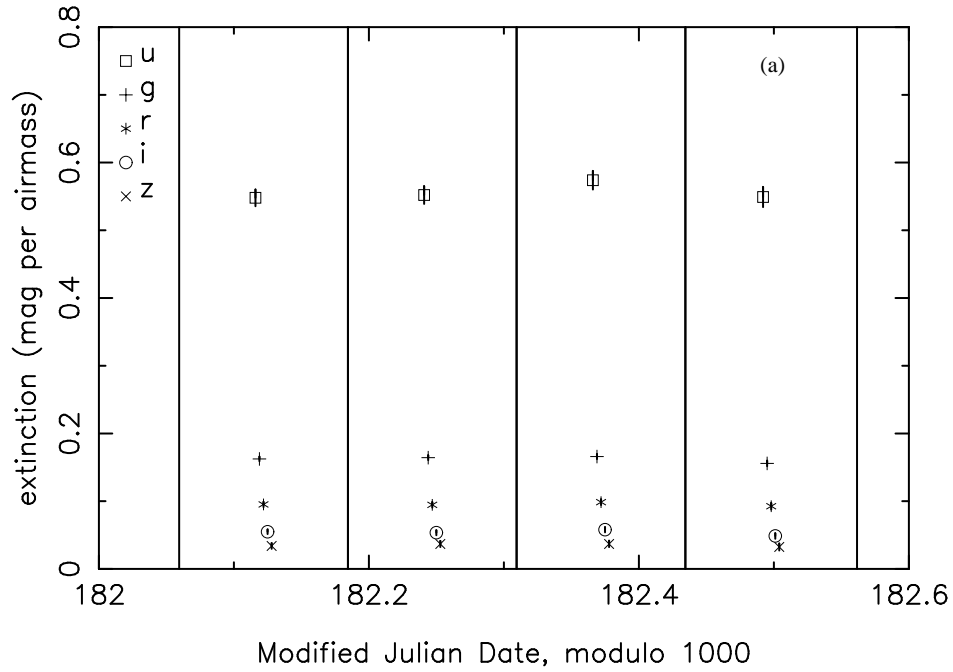
Extinction coefficients from photometric solution for 53501
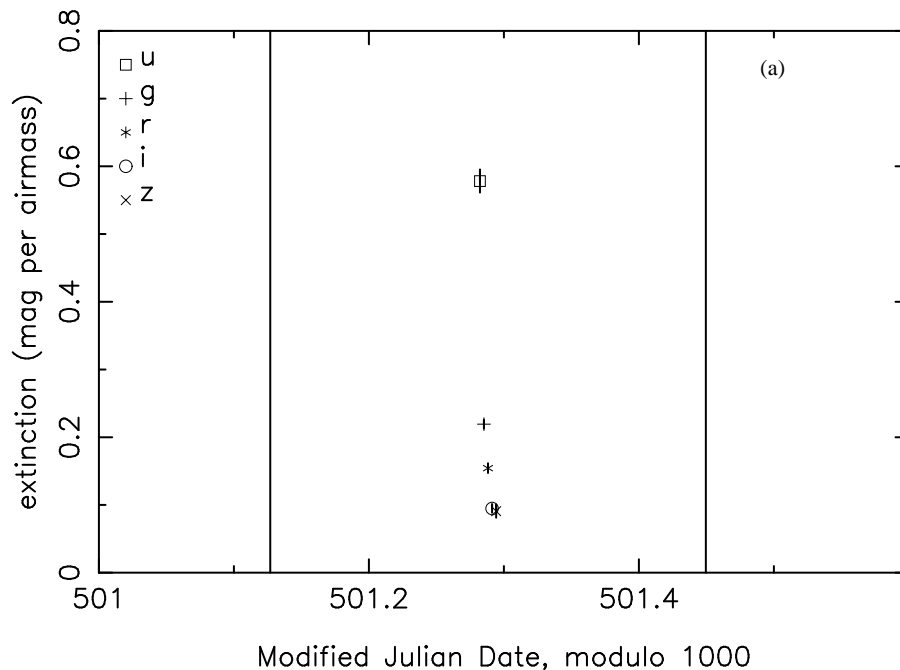


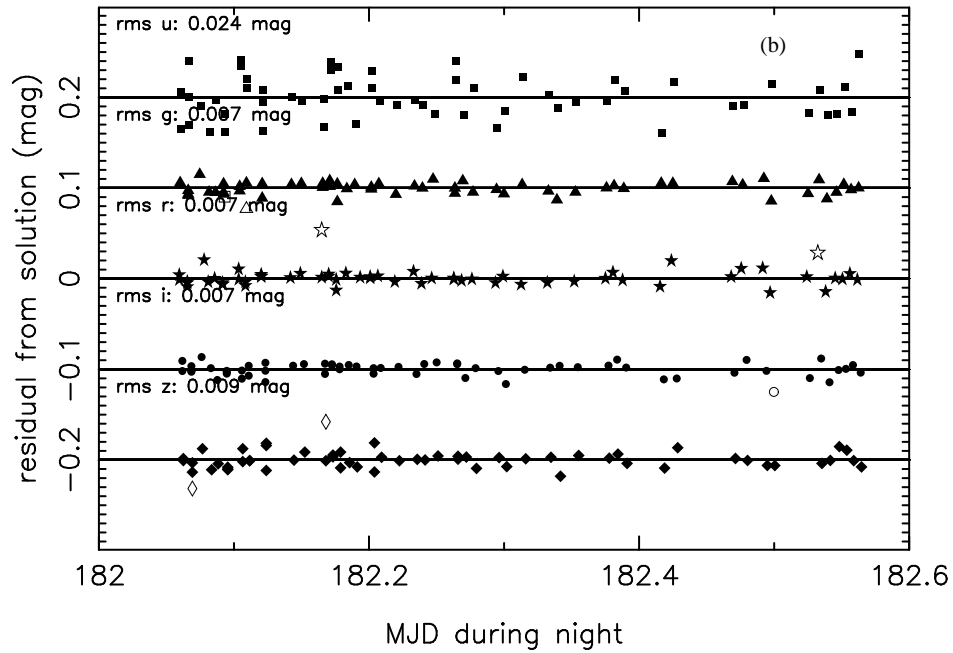mag residuals for primary standard stars in run 53501



**Fig. 8** A sampling of the quality assurance plots output by `excal` for the PT data taken on the night of MJD 53501: (a) first-order extinctions ($k$ coefficients) vs. time for each of the five passbands, and (b) magnitude residuals for the $u'g'r'i'z'$ standard stars observed over the course of the night (the zero lines are staggered by 0.1mag offsets in order to include the residuals from all five filters on the same plot). Note that, in (b), solid symbols denote the observations that were included in the solution, whereas open symbols denote the observations that were removed from the solution.

Fig. 9    The same `excal` quality assurance plots as in Figure 8, but for the USNO-1.0m data taken on the night of MJD 51182, in which the $k$ terms were solved for in 3-hour time blocks.

**Table 3**  Instrumental Color Terms For the PT (`excal`)

| <MJD> | $b(u')$ | $b(g')$ | $b(r')$ | $b(i')$ | $b(z')$ |
|---|---|---|---|---|---|
| Old $u'g'r'i'z'$ filters | | | | | |
| 51551 | 0.001 | 0.023 | 0.024 | 0.028 | 0.002 |
| 51580 | 0.001 | 0.025 | 0.025 | 0.029 | 0.002 |
| 51609 | 0.001 | 0.024 | 0.024 | 0.028 | 0.002 |
| 51639 | 0.001 | 0.023 | 0.024 | 0.028 | 0.002 |
| 51668 | 0.001 | 0.015 | 0.022 | 0.025 | 0.002 |
| 51698 | 0.001 | -0.003 | 0.017 | 0.017 | 0.002 |
| 51727 | 0.001 | -0.015 | 0.014 | 0.012 | 0.002 |
| 51786 | 0.001 | -0.015 | 0.014 | 0.012 | 0.002 |
| 51815 | 0.001 | 0.008 | 0.020 | 0.021 | 0.002 |
| 51845 | 0.001 | 0.020 | 0.023 | 0.027 | 0.002 |
| 51874 | 0.001 | 0.027 | 0.025 | 0.029 | 0.002 |
| 51904 | 0.001 | 0.032 | 0.026 | 0.031 | 0.002 |
| 51934 | 0.001 | 0.034 | 0.027 | 0.032 | 0.002 |
| 51964 | 0.001 | 0.033 | 0.027 | 0.032 | 0.002 |
| 51993 | 0.001 | 0.031 | 0.026 | 0.031 | 0.002 |
| 52023 | 0.001 | 0.024 | 0.024 | 0.028 | 0.002 |
| 52052 | 0.001 | 0.014 | 0.022 | 0.024 | 0.002 |
| 52082 | 0.001 | -0.004 | 0.017 | 0.017 | 0.002 |
| 52111 | 0.001 | -0.016 | 0.014 | 0.012 | 0.002 |
| New $u'g'r'i'z'$ filters | | | | | |
| $\geq$52140 | 0.001 | -0.041 | 0.009 | 0.010 | 0.002 |

**Table 4**  PT Standard Star Color Ranges (`excal` & `kali`)

| | color |
|---|---|
| | $0.70 \leq (u' - g')_{\rm o} \leq 2.70$ |
| | $0.15 \leq (g' - r')_{\rm o} \leq 1.20$ |
| | $-0.10 \leq (r' - i')_{\rm o} \leq 0.60$ |
| | $-0.20 \leq (i' - z')_{\rm o} \leq 0.40$ |

(which is measured by the atmospheric extinction term), can vary significantly over the course of a single night. Therefore, `excal` has the option to solve for the extinction in blocks of time that cover a night. In processing the original $u'g'r'i'z'$ standard star network, typically 3-hour blocks were used; in standard PT operations, typically the block size is set to 15 hours or more, in order to solve for only a single nightly extinction in each passband. Instrumental color terms and second-order (color×airmass) extinctions may also solved for, although generally multiple nights of data are needed to determine these with any confidence, so their values are usually set to pre-determined defaults. Uncalibrated candidate standard stars (i.e., stars which are believed to be non-variable but do not have previously determined $u'g'r'i'z'$ magnitudes) can also be used in the least squares solution as extinction standards; a useful output of the least squares routine is an estimate of their calibrated $u'g'r'i'z'$ magnitudes.

The photometric equations solved for by `excal` have, for a given filter $x$ and color index $x - y$, the following generic form:

$$
\begin{aligned}
x_{\rm inst} = {}& x_{\rm o} + a_x + k_x X \\
& + b_x[(x-y)_{\rm o} - (x-y)_{\rm o,zp}] \\
& + c_x[(x-y)_{\rm o} - (x-y)_{\rm o,zp}][X - X_{\rm zp}], \quad (1)
\end{aligned}
$$

where $x_{\rm inst}$ is the measured instrumental magnitude in filter $x$, $x_{\rm o}$ is the extra-atmospheric magnitude, $(x - y)_{\rm o}$ is the extra-atmospheric color, $a_x$ is the nightly zero point, $k_x$ is the first order extinction coefficient, $b_x$ is the system transform coefficient, $c_x$ is the second order (color) extinction coefficient, and $X$ is the airmass of the observation. $X_{\rm zp}$ and $(x - y)_{\rm o,zp}$ are zeropoint constants for the airmass $X$ and the color index $(x - y)$, respectively.

For standard PT reductions, the filter bands are linked to the color indices shown in Table 1, the color zeropoint constants are set to the values shown in Table 2, and $X_{\rm zp}$ is set to 1.3 (roughly the average airmass of the standard star observations). Furthermore, since their values are all very small and since removing them simplifies the fits to the data, the second-order extinction coefficients (the $c_x$'s) are all set to zero for standard PT reductions.

Note that the choice of which color index is linked with which filter band is an option in `excal`. For instance, in our effort to extend the $u'g'r'i'z'$ standard star network into the southern hemisphere (see § 5), we link the $i'$ band to the $(i' - z')$ color index rather than to the $(r' - i')$ color index used in the standard PT reductions, in order to maintain consistency with the photometric equations used in establishing the original $u'g'r'i'z'$ standard star system (Smith et al. 2002).

The photometric equations are solved iteratively, performing the following loop:

1. The photometric equations are fed the current estimates for the extra-atmospheric magnitude, colors, and photometric coefficients (e.g., for the $g'$ passband, these would be $g'_{\rm o}$, $(g' - r')_{\rm o}$, $a_g$, $b_g$, $c_g$, and $k_g$). For the first iteration of this loop, initial estimates for these parameters are fed into the equations.

2. The photometric equation for each of the passbands is solved in turn. This is done for all 5 passbands. If any stars (e.g., extinction standards) are having their magnitudes (e.g., $g'_{\rm o}$) solved for, their colors (e.g., $(g' - r')_{\rm o}$) are kept fixed at the values they had at the first step of this loop. (Having the colors change as their magnitudes in each filter are updated as one goes from one filter's equation to the next has been found to yield unstable solutions.)

3. Next, after the equations for all 5 passbands have been solved, if any extinction star magnitudes, are being solved for, their colors must be updated and saved for the next iteration.

4. If `excal` is being run interactively (a rare occurrence nowadays for PT processing; see § 4), then the residuals from the photometric solution are displayed to the screen, in each passband, and the user is allowed to discard stars from the solution (or add back in stars previously discarded).
   If the user *does* add/remove any star to/from the solution, `excal` returns immediately back to the top of the loop and starts again; otherwise, `excal` exits out of the loop.

5. If `excal` is being run non-interactively, it sigma-clips the outliers in the residuals and returns to the top of the loop. In this case, the number of iterations of this loop is controlled by an adjustable parameter. For normal PT operations, the clipping is done at the $2.5\sigma$ level, and the loop performs 3 iterations.

One can also choose to fix any of the photometric coefficients to a preset value and *not* solve for it. For instance, for the PT, we set the instrumental color terms to the preset values shown in Table 3 (linearly interpolating between MJDs as needed). Note that, up through July 2001, the PT had a set of $u'g'r'i'z$ filters which showed a fairly strong seasonal variations; the current set of PT $u'g'r'i'z'$ filters, installed in August 2001, have much more stable transmissions.

For PT reductions, where the prime focus is providing secondary patch stars calibrated on the SDSS 2.5m $ugriz$ system, the set of standard stars used in the fits to the photometric equations are constrained to a set of relatively narrow color ranges (shown in Table 4). Only standard stars that fall within all four of these color ranges are used, for, within these narrow ranges, the transformation from the USNO $u'g'r'i'z'$ system to the SDSS $ugriz$ system is best determined and known to be very linear.

Finally, `excal`, like `mtFrames`, also outputs quality assurance plots for the night processed. Figure 8 shows quality plots for a night of PT data (MJD 53501) in which the first-order extinctions ($k$-terms) were solved for in one long (15-hour) time block that covers the whole night. Figure 9 shows quality plots for a night of USNO-1.0m data (MJD 51182) in which the $k$ first-order extinctions where solved for in shorter (3-hour) time blocks.

Figures 8a and 9a show the first-order extinctions for the two nights in question; Figures 8b and 9b, the residuals all of the standard stars observed over the course of each of these two nights. For PT reductions, we consider a night photometric if the rms residuals are $\sigma_{u'} \leq 0.040$ mag, $\sigma_{g'} \leq 0.025$ mag, $\sigma_{r'} \leq 0.025$ mag, $\sigma_{i'} \leq 0.025$ mag, *and* $\sigma_{z'} \leq 0.040$ mag.

## 2.4 `kali`

The last package used in normal operations, `kali`, performs the astrometric calibration of the secondary and applies the photometric solutions produced by `excal` to the secondary patch instrumental magnitudes. As noted above, these secondary patch fields, which are observed by the PT, are later scanned over by the imaging camera on the SDSS 2.5m telescope. Thus, they act as calibration transfer fields to set the photometric zeropoints for the imaging camera data. The `kali` package can also be applied to calibrate manual, or target-of-opportunity, fields observed during a night.

Astrometry is performed using a triangle matching technique based upon the one used by the Faint-Object Classfi-

cation and Analysis System (FOCAS; Valdes et al. 1995).[6] For standard PT processing, finding charts extracted from the Guide Star Catalog 1.1 (Lasker et al. 1990) are used for the matching. For telescopes with smaller fields-of-view (e.g., the USNO-1.0m and the CTIO-0.9m; see § 5), however, the deeper (and hence more densely populated) Guide Star Catlogue 2.2[7] is sometimes necessary to obtain a good astrometric solution for a given field.

`kali` outputs the photometry for the secondary patches both in the USNO $u'g'r'i'z'$ system and in the SDSS $ugriz$ magnitudes. `kali` first applies the $u'g'r'i'z'$ photometric solutions from `excal` to the instrumental magnitudes of the secondary patches. This step is performed iteratively, until the calibrated $u'g'r'i'z'$ magnitudes have converged. To convert from the USNO $u'g'r'i'z$ system to the SDSS 2.5m telescope's $ugriz$ system, `kali` applies the following transformation equations:

$$u_{\mathrm{o}} = u_{\mathrm{o}}' \tag{2}$$
$$g_{\mathrm{o}} = g_{\mathrm{o}}' + 0.060 \times [(g' - r')_{\mathrm{o}} - 0.53] \tag{3}$$
$$r_{\mathrm{o}} = r_{\mathrm{o}}' + 0.035 \times [(r' - i')_{\mathrm{o}} - 0.21] \tag{4}$$
$$i_{\mathrm{o}} = i_{\mathrm{o}}' + 0.041 \times [(r' - i')_{\mathrm{o}} - 0.21] \tag{5}$$
$$z_{\mathrm{o}} = z_{\mathrm{o}}' - 0.030 \times [(i' - z')_{\mathrm{o}} - 0.09]. \tag{6}$$

Strictly speaking, the SDSS $ugriz$ magnitudes output by `kali` only apply within the narrow color ranges described by Table 4, although they are generally accurate for a much broader range, at least for normal stars (e.g., stars showing no strong emission features in the their spectra) blueward of the M0 spectral type (see, for example, Fig. 7 and 8 of Rider et al. 2004).

Further, like `mtFrames` and `excal`, `kali` outputs some quality assurance plots for the night processed, a sampling of which is shown in Figures 10 and 11. Figure 10 shows how well the PT patches were matched to the the stars in the finding charts, and Figures 11a, b, and c show the $ugr$, $gri$, and $irz$ color-color diagrams, respectively, for the stars in the secondary patches observed on this night (the $ugr$ and $gri$ diagrams also show a stellar locus (Lenz et al. 1998) for comparison).

Finally, `kali` automatically tags the quality of the photometry within individual secondary and manual patches by monitoring the position of certain features in each patch's color-color diagrams. For determining the quality of the photometry in the $griz$ bands, `kali` uses the location in $g' - r'$, $r' - i'$, $i' - z'$ space where the red and blue branches of the stellar locus cross — i.e., roughly where stars of spectral type M0 sit, which is at $g' - r' \approx 1.35$, $r' - i' \approx 0.50$, and $i' - z' \approx 0.25$; this is the so-called Zhed point test, a more refined version of which is described in detail by Ivezić et al. (2004). The quality of the $u$ band photometry is automatically tagged based upon the estimated $u' - g'$ color of stars in the blue branch at $g' - r' = 0.50$, which is $u' - g' \approx 1.45$.

---

[6] A standalone ANSI C version of this code can be obtained from http://spiff.rit.edu/match/.

[7] http://www-gsss.stsci.edu/gsc/gsc2/GSC2home.htm

## Percentage of stars matched in MT secondary fields for run 53501
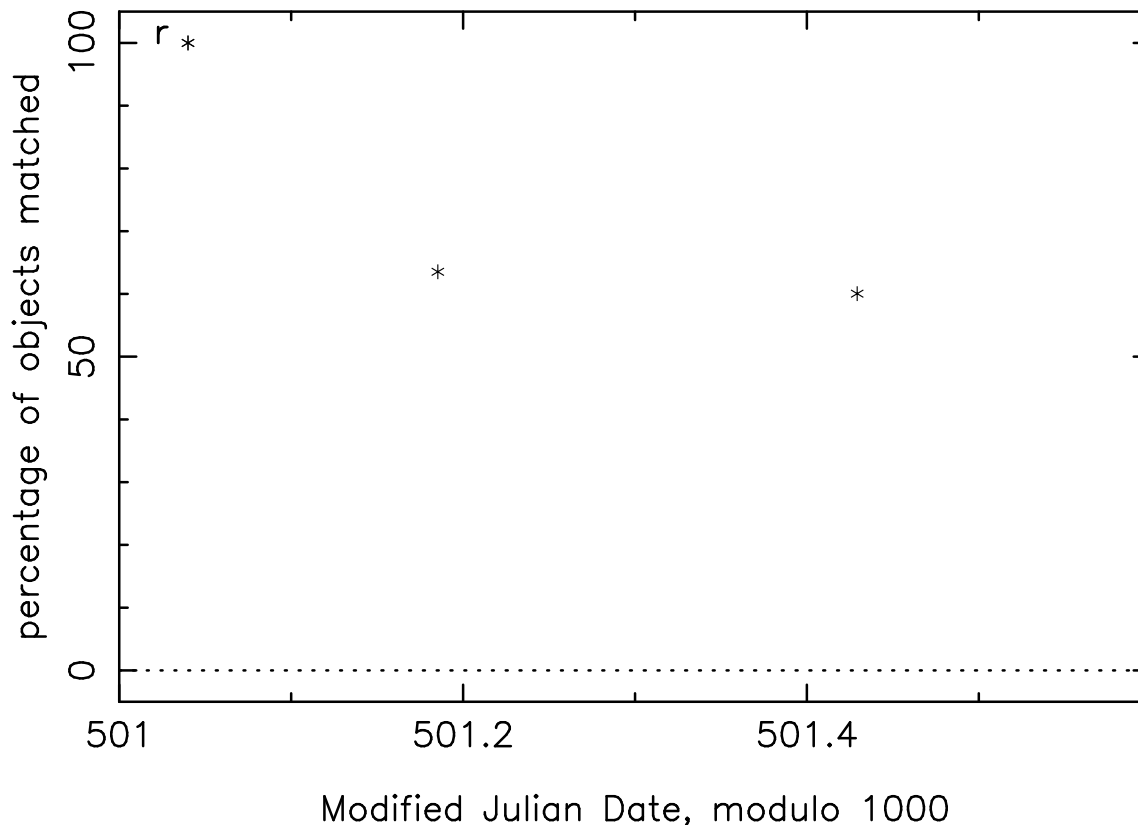


**Fig. 10** One of the quality assurance plots output by `kali` for the PT data taken on the night of MJD 53501: the percentage of stars detected in the $r'$-band matched to stars in the finding chart file for each of the secondary patches and manual target fields observed during the night (note that the finding chart file for each secondary patch and manual target field is extracted from the the Guide Star Catalog-I; Lasker et al. 1990).

### 2.5 Auxiliary Packages

In addition to the above four packages, which are used for normal night-to-night survey operations, there are two other packages — `solve_network` and `superExcal` — which were developed and used for setting up the $u'g'r'i'z'$ primary standard star network of Smith et al. (2002). These two packages are similar to `excal`, in that they invoke least squares routines to solve for the photometric parameters of a set of data and for the best-fit magnitudes of the primary standards. They differ from `excal` in that, whereas the main purpose of `excal` is the standard, single-night solution of the photometric equations during routine survey operations, the main purpose of `solve_network` and `superExcal` was to calibrate the SDSS standard star network. Both `solve_network` and `superExcal` use a single star to set the zeropoint for the photometric solution. For setting up the SDSS standard star network, this star was the F subdwarf BD+17°4708, whose magnitudes were *defined* to be $u' = 10.56$, $g' = 9.64$, $r' = 9.35$. $i' = 9.25$,

$z' = 9.23$, based upon the spectrophotometric calculations of Fukugita et al. (1996). Thus, BD+17°4708 sets the zeropoint for the entire standard star network.

Although they share the same goal and the same basic methodology, `solve_network` and `superExcal` do differ in some important respects, the most important being that the code for `solve_network` was constructed independently of that for `excal`, whereas `superExcal` was basically an outgrowth of `excal`. As a result, the separate results from these two different packages provide useful cross-checks on the final calibrations of the standard star system. Results and output of `solve_network` and `superExcal` can be found in Smith et al. (2002).

Finally, although not strictly an auxiliary package but more of an auxiliary mode of operations is the `MTPIPE` follow mode, which permits the near-realtime running of `mtFrames` and `excal` during data acquisition at the PT. `MTPIPE` in follow mode was used by the SDSS observers during the 2000–2001 time frame in conjunction with the `hoggpt` photometricity monitor (Hogg et al. 2001) in or-

Run 53501

(a)

Run 53501

(b)

Run 53501

(c)
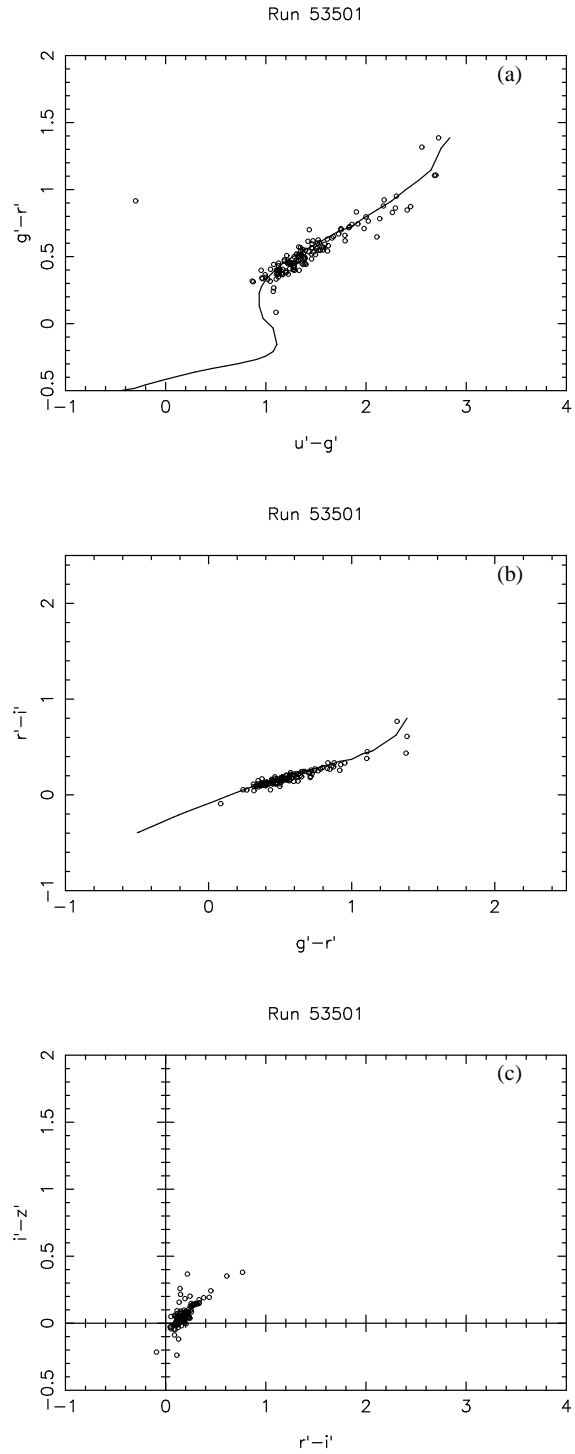
**Fig. 11** Color-color quality assurance plots output by `kali` for the PT data taken on the night of MJD 53501: (a) the combined $g - r$ vs. $u - g$ color-color diagram, (b) the combined $r - i$ vs. $g - r$ color-color diagram, and (c) the combined $i - z$ vs. $r - i$ color-color diagram for the stars in all the secondary patch and manual fields from the night. The lines in (a) and (b) show the $u'g'r'i'z'$ stellar loci (based on the stellar loci of Lenz et al. 1998).

der to track sky conditions over the course of a night. This functionality is nowadays completely handled by the dedicated `hoggpt` photometricity monitor.

## 3 Tests of `MTPIPE`

As a critical component in the photometric calibration of the SDSS, `MTPIPE` has undergone a variety of tests to ensure the validity of its outputs. Most of these tests have been aimed at the potentially trickier parts of `MTPIPE` — the image processing and aperture photometry in `mtFrames` and the photometric equations solver in `excal`.

A major test of `mtFrames` was accomplished by comparing its outputs with those of the `hoggpt` APO photometricity monitor (Hogg et al. 2001) for various nights of PT data. The `hoggpt` software was written completely independently of `mtpipe` in the data analysis language IDL.[8] It thus could act as an independent check of the data processing methods utilized in `mtFrames`. Overall, it was discovered that these pipelines created virtually identical master bias frames, master flat fields, and master fringes. Furthermore, for a given aperture size, the two pipelines yielded essentially indistinguishable aperture photometry. Plots comparing the aperture photometry from the two pipelines are shown in Figures 12, 13, and 14. In these plots, an aperture size of 7.43″radius is used on PT data from MJD 51639.

The basis of the `excal` photometric equations solver is an iterative non-linear matrix inversion routine which simultaneously solves for all parameters in each filter's photometric equation. To test this, a very stripped-down version of `excal` ("`subExcal`") was written which utilized a vanilla linear least squares line-fitting routine based upon the `LINFIT` routine of Bevington (1969) converted into the SDSS Tcl/`ASTROTOOLS` environment. `subExcal` does not solve for all parameters simultaneously, but first solves for the photometric zeropoint and the first order extinction (the $a$ and $k$ coefficients) by fitting a straight line to an equation of the form (taking the $g'$ filter as our example):

$$g'_{\mathrm{inst}} - g'_{\mathrm{o}} = a_g + k_g X, \tag{7}$$

(see Fig. 15), and then uses the values of the $a$ and $k$ terms thus obtained to solve for the $b$ coefficient by fitting another straight line to an equation of the form:

$$g'_{\mathrm{inst}} - g'_{\mathrm{o}} - a_g - k_g X = b_g(g' - r') \tag{8}$$

(see Fig. 16). In Table 5, we compare the output of `excal` against the output of `subExcal` for PT data from the night of MJD 51639. Note that in many cases, the results are indistinguishable, and in all cases the values differ by no more than $1\sigma$.

The `kali` package of `MTPIPE` is more or less straightforward. It performs astrometry on secondary patches, and the astrometry needs to be accurate enough for PT secondary patch stars to be cross-matched with stars in the SDSS 2.5m imaging camera data. Residuals in the astrometric solutions

---

[8] http://www.rsinc.com/

**Table 5** Comparison of `excal` and "`subExcal`" for MJD 51639

| Filter | Method | $a_{\mathrm{filter}}$ | $b_{\mathrm{filter}}$ | $k_{\mathrm{filter}}$ |
|--------|--------|-------|-------|-------|
| $u'$ | excal | $-19.286 \pm 0.042$ | $-0.011 \pm 0.014$ | $0.516 \pm 0.025$ |
|       | subExcal | $-19.318 \pm 0.037$ | $-0.011 \pm 0.013$ | $0.530 \pm 0.025$ |
| $g'$ | excal | $-20.668 \pm 0.019$ | $+0.026 \pm 0.007$ | $0.184 \pm 0.012$ |
|       | subExcal | $-20.673 \pm 0.021$ | $+0.026 \pm 0.007$ | $0.195 \pm 0.014$ |
| $r'$ | excal | $-20.578 \pm 0.021$ | $+0.033 \pm 0.015$ | $0.119 \pm 0.013$ |
|       | subExcal | $-20.573 \pm 0.022$ | $+0.033 \pm 0.015$ | $0.118 \pm 0.014$ |
| $i'$ | excal | $-20.194 \pm 0.020$ | $+0.026 \pm 0.023$ | $0.071 \pm 0.013$ |
|       | subExcal | $-20.188 \pm 0.020$ | $+0.025 \pm 0.022$ | $0.068 \pm 0.013$ |
| $z'$ | excal | $-19.162 \pm 0.026$ | $-0.025 \pm 0.029$ | $0.067 \pm 0.017$ |
|       | subExcal | $-19.164 \pm 0.025$ | $-0.025 \pm 0.029$ | $0.067 \pm 0.017$ |

(based against the Guide Star Catalog-I; Lasker et al. 1990) are typically less than $1''$ RMS in both RA×cos(DEC) and DEC, which is sufficient for the PT-2.5m cross-matches. Further, `kali` applies the photometric solutions from `excal` to the instrumental magnitudes of the secondary patches. This has been verified by manually applying the `excal` solutions to the instrumental magnitudes of the PT secondary patch data and comparing the results; the resulting differences are typically of the order of the roundoff error of the calculator/computer used for the manual computation.

Of course, in the final analysis, the true-end-to-end test of `MTPIPE` is the resulting quality of the SDSS photometric calibrations. As stated in the introduction of this paper, the rms errors measured over the several thousand square degrees that currently make up the SDSS imaging data set are $\approx 0.02$ mag (2%) rms over several thousand square degrees of sky in $g$, $r$, and $i$, and $\approx 0.03$ mag (3%) in $u$ and $z$ (Ivezić et al. 2004; Adelman-McCarthy et al. 2006).

In the future ($\S$ 5), `MTPIPE` will likely need to calibrate secondary patches at low Galactic latitudes for SDSS-II. How close to the Galactic Plane (i.e, at what stellar densities) can `MTPIPE` — which does aperture, not PSF, photometry — accurately calibrate these patches? One of us (CTR) is currently testing `MTPIPE` against `DAOPHOT` (Stetson 1987) for some low-Galactic-latitude PT fields.

## 4 The PT Factory

For the photometric calibration of the SDSS 2.5m imaging camera data, a method is needed for the timely, end-to-end processing of the PT data that is fully integrated and maintained within the official SDSS data processing environment at Fermilab. This need is fulfilled by the PT Factory, a term which applies to a suite of scripts that oversees the day-to-day processing and quality assurance of PT data at Fermilab. These scripts reside in the `dp` software data processing product, which is a collection of UNIX shell scripts and Tcl/`ASTROTOOLS` code that oversees the overall processing and quality assurance for 2.5m imaging, 2.5m spectroscopy, and PT data (Stoughton et al. 2002b).

Each morning, the PT Factory performs an `rsync`[9] copy of the previous night's PT data from APO to a local disk
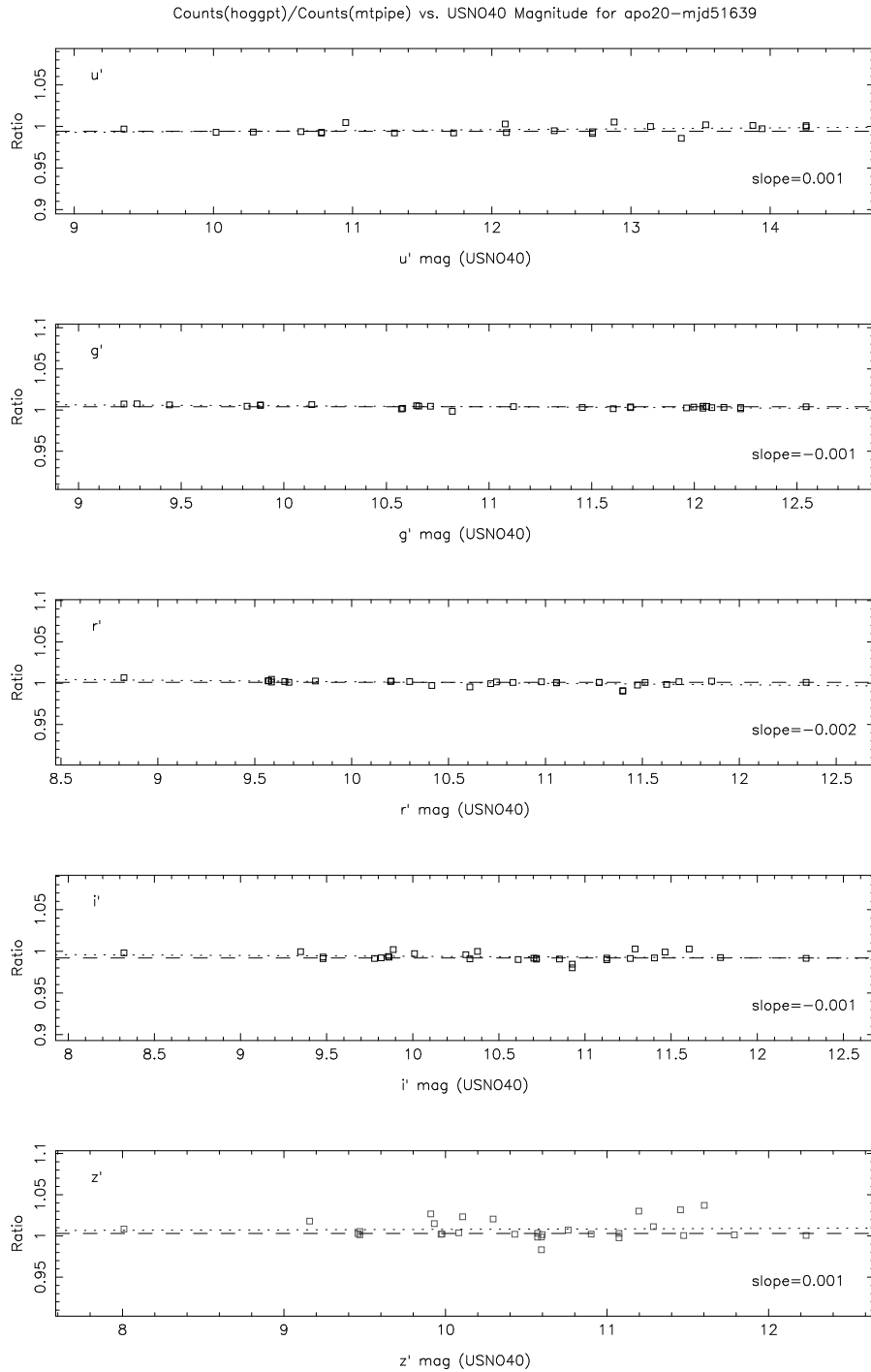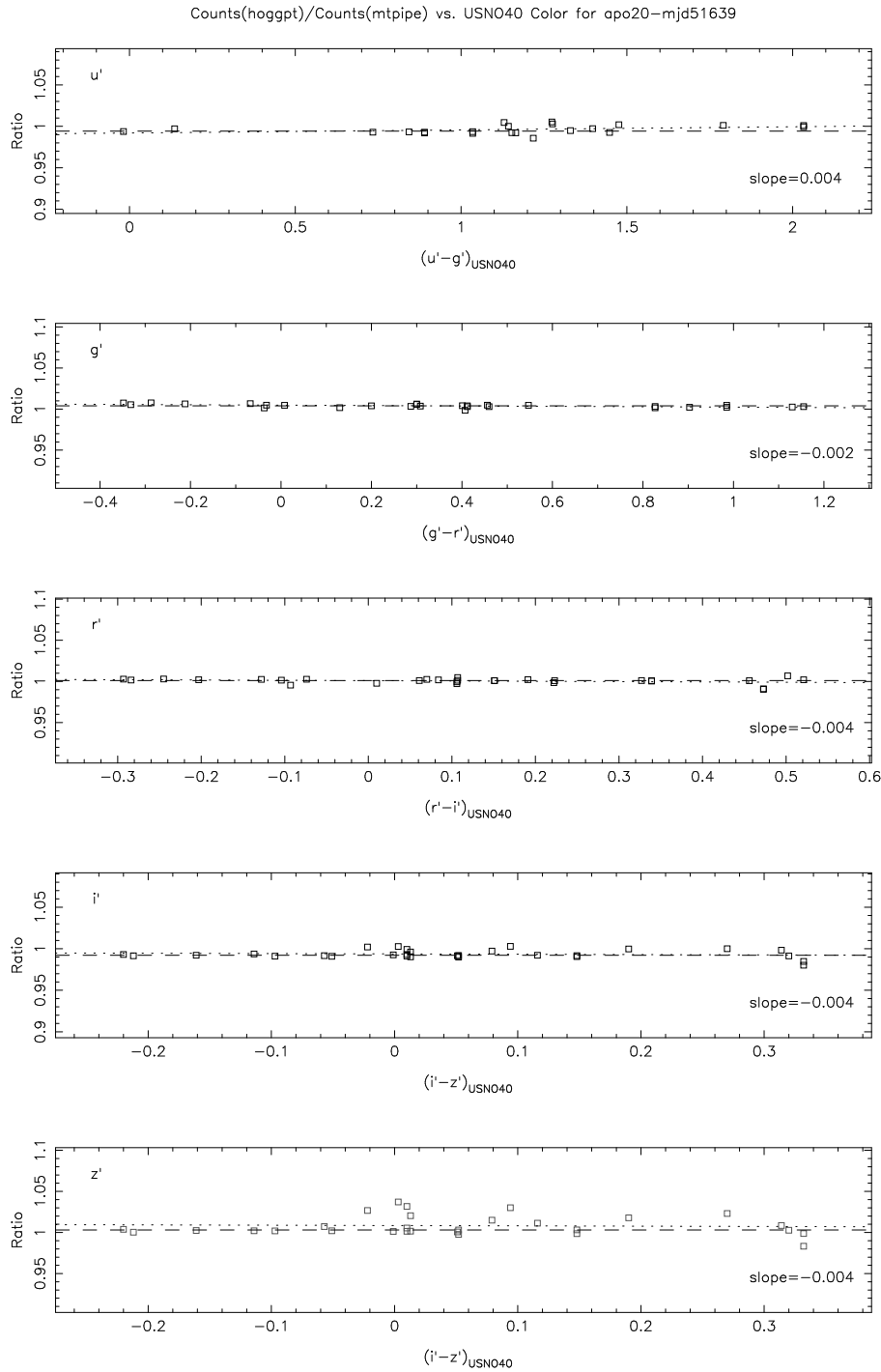
---

[9] http://rsync.samba.org/
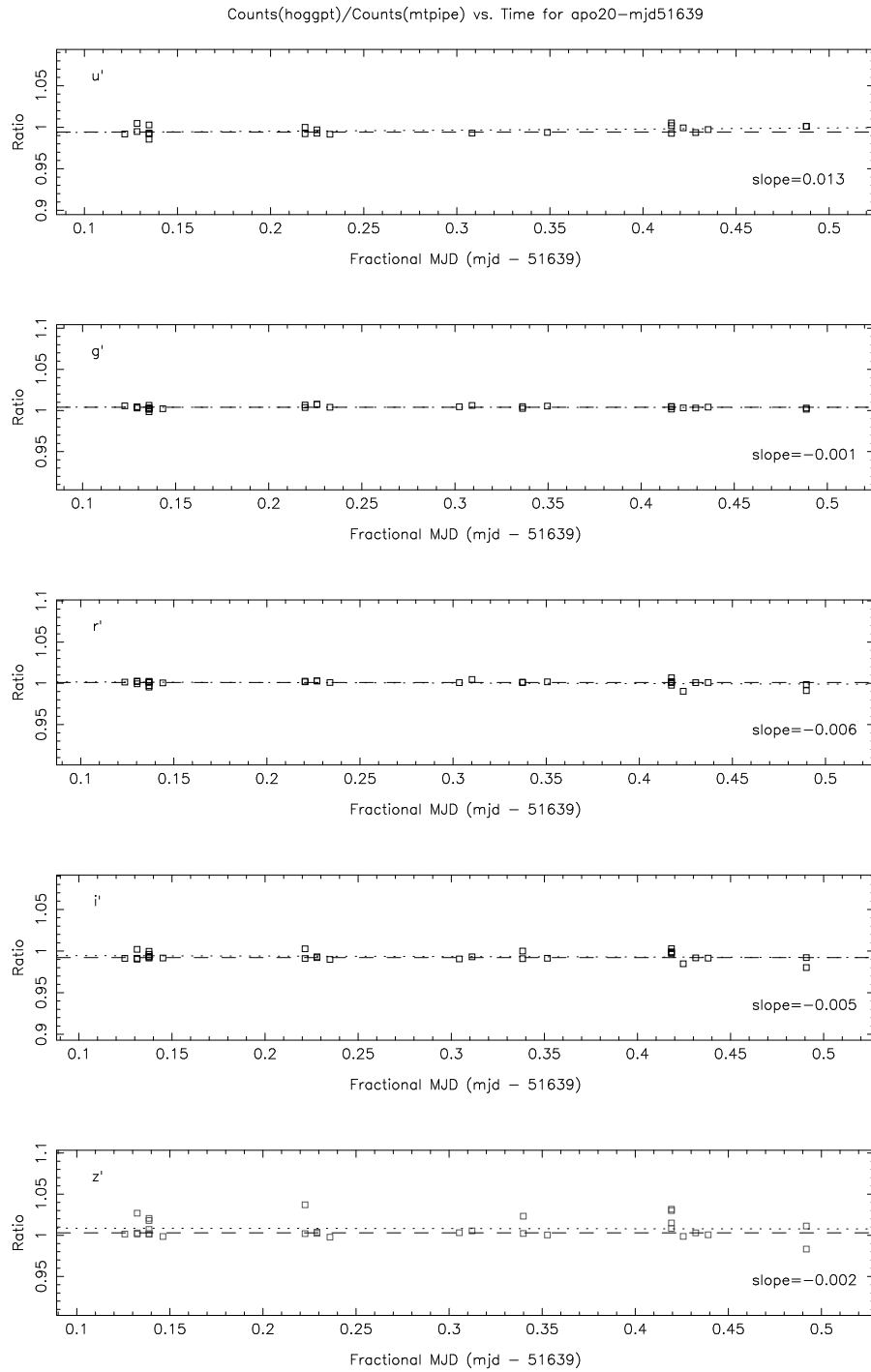
**Fig. 12** Comparison of aperture counts for standard stars from `hoggpt` and from `mtFrames` over the course of the night for the PT data from the night of MJD 51639. The dashed line in each panel is the median of the ratio of Counts(`hoggpt`)/Counts(`MTPIPE`) for data; its slope is flat. The dotted line in each panel is the best fit line to the data; its slope is noted in the panel's legend.

**Fig. 13** Comparison of aperture counts for the Smith et al. (2002) standard stars from `hoggpt` and from `mtFrames` vs. the USNO standard magnitude for the PT data from the night of MJD 51639. Dashed and dotted lines are as in Figure 12.

Counts(hoggpt)/Counts(mtpipe) vs. USNO40 Color for apo20-mjd51639

**Fig. 14** Comparison of aperture counts for the Smith et al. (2002) standard stars from `hoggpt` and from `mtFrames` vs. the USNO standard color for the PT data from the night of MJD 51639. Dashed and dotted lines are as in Figure 12.
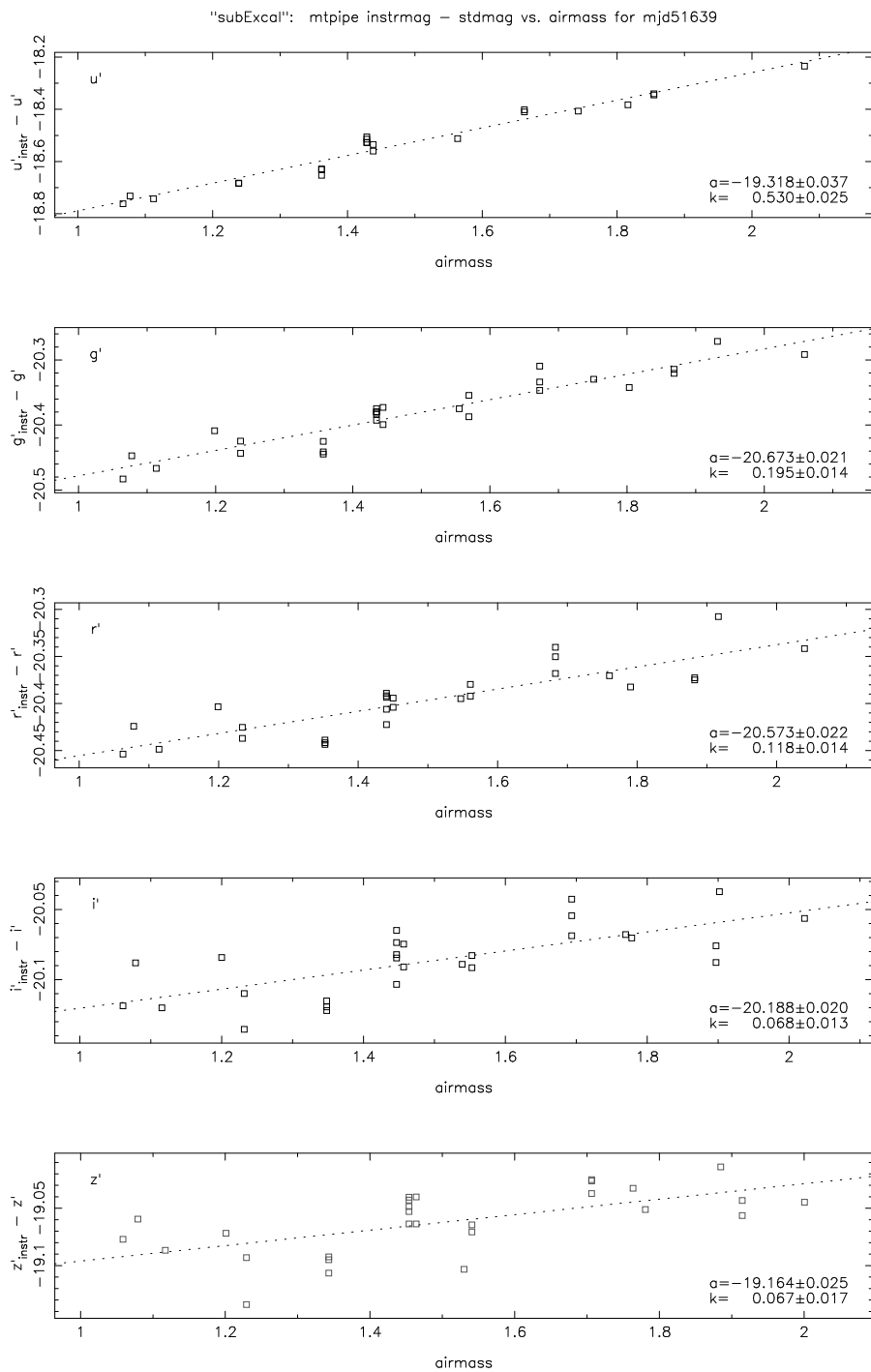
**Fig. 15** "subExcal" results for photometric zeropoints ($a$ terms) and first-order extinctions ($k$ terms) for the PT data from the night of MJD 51639. The dotted line in each panel shows the best fit line to the data. The values for the slope ($k$) and zeropoint ($a$) of the best fit line is shown in each panel's legend.
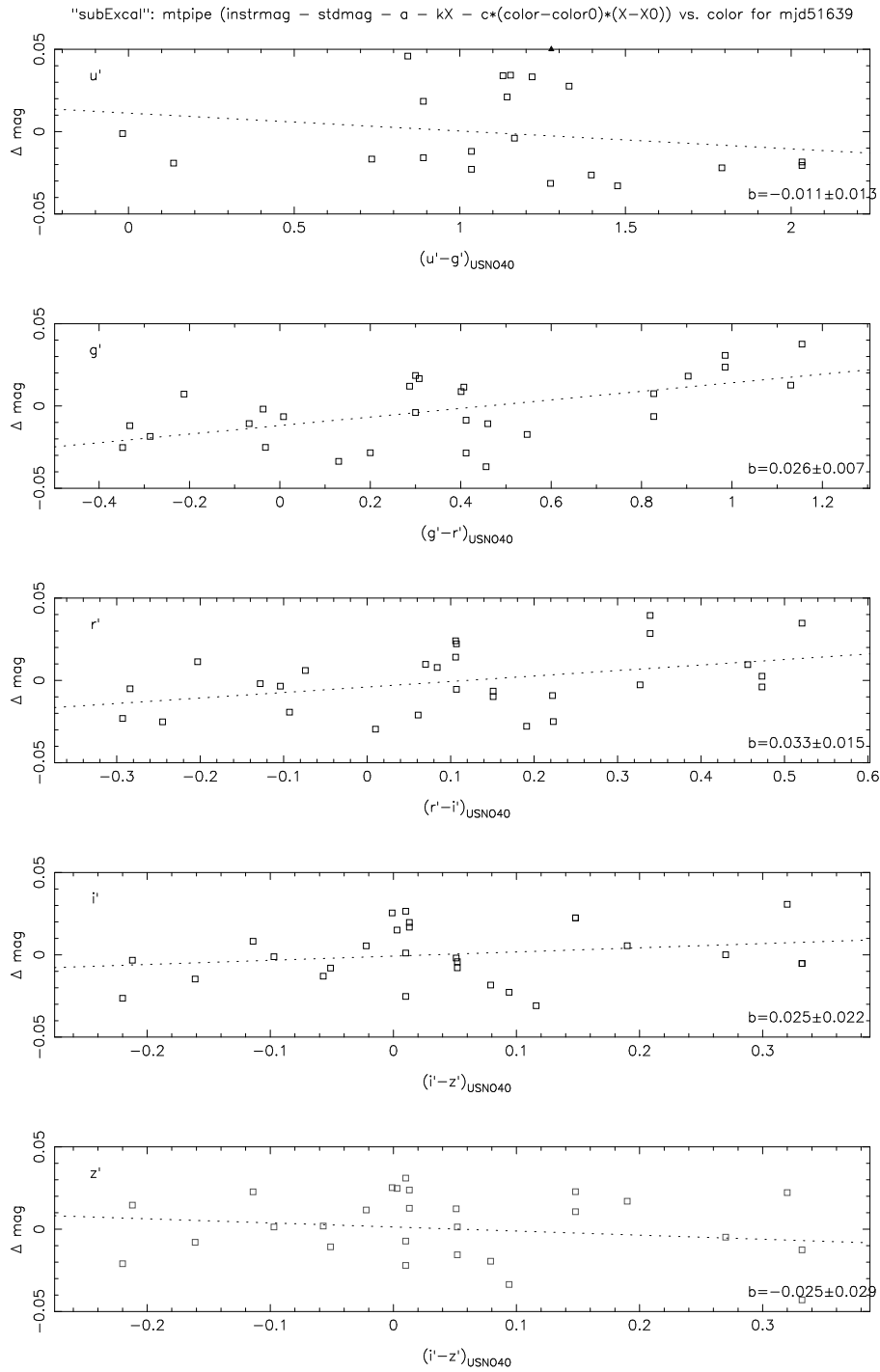
**Fig. 16** "subExcal" results for instrumental color (*b*) term coefficients for the PT data from the night of MJD 51639. The dotted line in each panel shows the best fit line to the data. The value for the slope (*b*) of the best fit line is shown in each panel's legend.

at Fermilab (typically $\sim$2 GB for a photometric night). The morning `rsync` also copies the night's images and log from the APO 10 micron All-Sky Camera[10] (Hogg et al. 2001); the log, which is a record of the sky rms for each all-sky camera image over the course of a night, is used by the PT Factory to flag and exclude from `mtpipe` processing any PT target images afflicted by clouds.

Once the PT Factory determines that the night's PT data have been completely transferred (typically by the early-to mid-afternoon of the same day), `MTPIPE` is automatically run on the data. Once `MTPIPE` has run to completion, there is a manual inspection step, in which a human checks over the quality assurance plots generated by `mtFrames`, `excal`, and `kali`. This manual inspection step exists to ensure that nothing unexpected occurred with either the raw data or with the data processing that was not already caught by `MTPIPE`'s automated quality assurance tests. If, as is generally the case, the night's processing passes the manual inspection step, the photometric solutions and survey-quality secondary patches are copied to a location on disk where `NFCALIB` expects to find them, and the contents of the night's reductions are loaded into a database and saved to a tape robot.

An additional input into the PT factory is the "ptlog" observer's report, which is e-mailed at the end of each night to a ptlog mailing list. This report contains summary comments on the night, including the sky conditions, which (if any) manual or special targets were observed, any issues with the PT hardware or observing software, and any other comments that might be relevant to either the PT data processing or to the PT operations. The ptlog is read each morning, and its contents are used in deciding whether any manual intervention of the PT Factory is needed for that night's data. As such, it provides an essential link between the observers at APO and the data processors at FNAL.

A final step of PT processing, not strictly part of the PT Factory, is updating the secondary patch database maintained at APO. This database keeps track of which secondary patches have been observed, which have not been observed, and which of the observed patches have been determined by the PT Factory to be of survey quality. It also keeps track of the observing priority of the secondary patches. This database therefore serves as essential feedback to the observers regarding the secondary patch observing priorities for a given dark run or even a given night.

## 5 Other SDSS-related Projects using `MTPIPE`

Since the inception of the SDSS observing effort on the PT, we were aware that `MTPIPE` would enable additional projects to be undertaken. Initially, these were centered on use of the PT during bright time, but later it became apparent that other telescopes could be used with modification of

the `preMtFrames` code and creation of additional input parameter files.

Early in the SDSS we recognized the usefulness of open star clusters as potential calibration fields for the main survey, as well as being good science targets in their own right. This led to the development of a star cluster project in the $u'g'r'i'z'$ filter system. Also, shortly after the establishment of the original $u'g'r'i'z'$ standard star network (Smith et al. 2002), we began to receive requests for southern hemisphere standard stars. These requests led us to develop a southern $u'g'r'i'z'$ standard stars project which was undertaken as an NOAO Survey Program. Further, as we reached the point where we could see the end of the SDSS proper, development of survey extension strategies were pursued by the collaboration. The PT and the `MTPIPE` software are integral to the support of these extension efforts.

In the rest of this section, we will briefly discuss each of the project areas that are enabled by this unique calibration software, and point to references for additional information.

### 5.1   Southern $u'g'r'i'z'$ Standards Project

Due to the nature and location of the SDSS, the bulk of the initial set of standard stars to calibrate the survey were placed in the northern hemisphere and on the equator (Fig. 1). As part of the NOAO Surveys Program,[11] a group of us was granted time on the CTIO-0.9m over the 2000-2004 time period in order to establish a network of $u'g'r'i'z'$ standard stars in the southern hemisphere (see Fig. 1). Processing and analysis of these data are nearly complete, and we are targetting the second-half of 2006 for release of the bulk of the data. (An initial data release for standard stars in the Chandra Deep Field South appeared in Smith et al. 2003.) As the processing and analysis is completed, results will be made available on our publicly accessible website.[12]

### 5.2   $u'g'r'i'z'$ Open Clusters Project

One of the most powerful tools available in astrophysics for exploring and testing theories of star formation, stellar and galactic evolution, and the chemical enrichment history of the Galaxy is the study of open star clusters. Therefore, a group of us embarked on a survey of (mostly) southern hemisphere open star clusters using the $u'g'r'i'z'$ filter system on small telescopes. This project had as its original goal to verify the SDSS calibration scheme. This goal has since evolved. Current plans for observing star clusters in the SDSS filter system now include: (1) their potential use in calibrating the SDSS extension programs, and (2) creating a large uniform imaging survey of clusters similar to the WIYN Open Cluster Survey (WOCS) (see Mathieu 2000).

In the first of our cluster papers (Rider et al. 2004), we present results for NGC 2548. We chose this particular cluster because we had observations of it using three telescopes:

---

[10] http://hoggpt.apo.nmsu.edu/irsc/tonight/

[11] http://www.noao.edu/gateway/surveys/programs.html
[12] http://www-star.fnal.gov/

the CTIO Curtis-Schmidt, the PT, and, most importantly, the USNO-1 m, the telescope with defines the $u'g'r'i'z'$ photometric system (Smith et al. 2002). A second cluster paper (Moore et al. 2006) has been submitted and addresses NGC 6134 and Hogg-19. Further papers are in preparation. In all, we have data in hand for $\approx$100 open clusters.

These data may be used to verify the recent age and metallicity models of Girardi et al. (2004) and the prior work of Lenz et al. (1998), and to verify and expand upon the $u'g'r'i'z'$ to $UBVR_cI_c$ transformations presented in the standard star paper (Smith et al. 2002). Rodgers et al. (2006) is taking another look at these filter system transformations for main sequence stars in an effort to sort out luminosity class effects.

### 5.3 SDSS-II

The SDSS officially ended on 2005 June 30. The SDSS-II is a 3-year extension of the SDSS beyond this date, and is composed of three parts:

1. The Legacy Survey, which will fill in a gap in the SDSS imaging and spectroscopic coverage of the Northern Galactic Cap due to worse-than-expected weather conditions during the five years of the original SDSS.
2. The Sloan Extension for Galactic Understanding and Exploration, or SEGUE, which will image about 3500 sq deg of sky — mostly at Galactic latitudes of $|b^{II}| < 30°$ — and measure spectra to determine abundances and radial velocities of a quarter of a million stars, in order to study the structure and evolution of the Milky Way (Newberg et al. 2004).
3. The SDSS-II Supernova Survey, which will image 250 sq deg along the Celestial Equator every two nights during the Autumns of 2005-2007, with the aim of obtaining well-sampled, well-calibrated, multi-band lightcurves for 200 Type Ia supernovae in the redshift "desert" $z = 0.1 - 0.35$ (Frieman et al. 2004; Sako et al. 2005).

The PT and MTPIPE are playing an important role in all three of these components of the SDSS-II. First of all, since it is basically a continuation of the original SDSS within the original survey borders, the Legacy component of SDSS-II continues to benefit from the use of MTPIPE reductions of PT secondary patches as part of the general photometric calibration strategy of the 2.5m imaging camera data.

Likewise, the 2.5m imaging scans for SEGUE also uses MTPIPE reductions of PT secondary patches located within the SEGUE survey area (see Fig. 2). But the PT and other small telescopes (like the USNO-1.0m) have an even bigger role to play in SEGUE. One of the major thrusts of SEGUE is the SEGUE Open Cluster Survey. This is a wide-field imaging program with limited spectroscopic follow-up within SDSS-II. While the imaging program will not go as faint as the WOCS (see Mathieu 2000), we will observe almost an order of magnitude more clusters than the WOCS. Directed pointings for specific calibration targets and for the brighter stars of the clusters will be undertaken with

the smaller telescopes, and those data will be reduced with MTPIPE.

Finally, the PT and MTPIPE have a role to play in the Supernova component of the SDSS-II. In this case, the role has less to do with photometric calibrations — since the primary Supernova strategy is to use differential photometry of repeat 2.5m imaging scans against previously calibrated areas of the sky scanned by the original SDSS survey — but more of a role in followup observations. Here, the PT will be able to follow the light curves of the brighter candidate Type Ia supernovae detected by the main SDSS-II Supernova Survey during those times when 2.5m telescope time is allotted either to the Legacy survey or to SEGUE, and MTPIPE will be able to process these PT observations.

## 6 The Future

MTPIPE is a mature and stable data processing pipeline. The last major revision — from v7.4 to v8.0 occurred over four years ago (on 2002 April 22). As noted in § 2, the current version is v8.3, and the changes since v8.0 have been mostly cosmetic and have generally dealt with the smooth running of the PT Factory (§ 4). This being the case, what is the future of MTPIPE?

There are, of course, many relatively small changes to MTPIPE that could yield incremental improvements in the final output and to the photometric calibrations of the SDSS. These include updates to the de-fringing code in mtFrames and continued improvements to the automated quality assessment of secondary patches for the PT Factory. Also, improving the compatibility of the output of MTPIPE with other astronomical data packages would be a plus. Along these lines, adding World Coordinate System (WCS; Calabretta & Greisen 2002; Greisen & Calibretta 2002) keywords to the FITS headers of MTPIPE corrected images is high on the list of priorities. (Currently, there is a standalone Tcl/ASTROTOOLS script to do this, but it has yet to be fully incorporated into MTPIPE.)

A larger task that may be ahead for MTPIPE is how to deal with crowded field photometry. mtFrames is an aperture photometry code, but many of the science projects that currently use or plan to use MTPIPE involve crowded fields — in particular, star clusters (§ 5). Furthermore, the photometric calibration SDSS-II/SEGUE scans may require the placement of SEGUE secondary patches at very low Galactic latitude. With the task of crowded field photometry in mind, then, we are investigating the possibility of adding a toggle switch to mtFrames which would allow one to choose to run a PSF-fitting photometry package like DAOPHOT (Stetson 1987) or DoPHOT (Schechter et al. 1993) on corrected frames output by mtFrames; a new script, which would be run after mtFrames, would then package the resulting DAOPHOT/DoPHOT output into an excal-/kali-ingestible format.

# References

Abazajian, K., et al.: 2003, AJ 126, 2081 (DR1)

Abazajian, K., et al.: 2004, AJ 128, 502 (DR2)

Abazajian, K., et al.: 2005, AJ 129, 1755 (DR3)

Adelman-McCarthy, J., et al.: 2006, ApJS 162, 38 (DR4)

Allen, R.J., Ekers, R.D., Terlouw, J.P.: 1985, in Data Analysis in Astronomy, Ettore Majorana International Science Series, ed. V. Di Gesù, L. Scarsi, P. Crane, J.H. Friedman, and S. Levialdi, (New York: Plenum Press), p.271

Bertin, E., Arnouts, S.: 1996, A&AS 117, 393

Bevington, P.R.: 1969, *Data Reduction and Error Analysis for the Physical Sciences*, (New York: McGraw-Hill, Inc.)

Calabretta, M.R., Greisen, E.W.: 2002, A&A 395, 1077

Eisenstein, D.J., et al.: 2001, AJ 122, 2267

Frieman, J., Adelman-McCarthy, J., Barentine, J., et al.: 2004, American Astronomical Society Meeting Abstracts 205, #120.01

Fukugita, M., Ichikawa, T., Gunn, J.E., Doi, M., Shimasaku, K., Schneider, D.P. 1996: AJ 111, 1748

Girardi, L., Grebel, E.K., Odenkirchen, M., Chiosi, C.: 2004, A&A 422, 205

Grado, A., et al.:2004, AN , 325, 601

Greisen, E.W., Calabretta, M.R.: 2002, A&A 395, 1061

Grosbøl, P.: 1989, Reviews in Modern Astronomy 2, 242

Guidorzi, C., et al.: 2006, PASP 118, 288

Gunn, J.E., Carr, M., Rockosi, C., Sekiguchi, M., et al.: 1998, AJ 116, 3040

Gunn, J.E., Siegmund, W.A., Mannery, E.J., et al.: 2006, AJ 131, 2332

Hogg, D.W., Schlegel, D.J., Finkbeiner, D.P., Gunn, J.E.: 2001, AJ 122, 2129

Irwin, M, Lewis, J.: 2001, New Astronomy Reviews 45, 105

Ivezić, Ž., Lupton, R.H., Schlegel, D., Boroski, B., Adelman-McCarthy, J., Yanny, B., Kent, S., Finkbeiner, D., Padmanabhan, N., et al.: 2004, AN 325, 583

Landolt, A.U.: 1973, AJ 78, 959

Landolt, A.U.: 1983, AJ 88, 439

Landolt, A.U.: 1992, AJ 104, 372

Landolt, A.U.: in preparation

Lasker, B.M., Sturch, C.R., McLean, B.J., Russell, J.L., Jenkner, H., Shara, M.M.: 1990, AJ 99, 2019

Lenz, D.D., Newberg, H.J., Rosner, R., Richards, G.T., Stoughton, C.: 1998, ApJS 119, 121

Lupton, R., Gunn, J.E., Ivezić, Z., Knapp, G.R., Kent, S., Yasuda, N.: 2001, in ASP Conf. Ser. 238, Astronomical Data Analysis Software and Systems X, ed. F. R. Harnden, Jr., F. A. Primini, and H. E. Payne (San Francisco: Astr. Soc. Pac.), p. 269

Lupton, R.H.: 2006, in preparation

Mathieu, R.D.: 2000, ASP Conf. Ser. 198: Stellar Clusters and Associations: Convection, Rotation, and Dynamos, 517

Moore, D.C., Tucker, D.L., Smith, J.A., Stoughton, C., Rider, C.J., Allam, S.S., Rodgers, T.C.: 2006, AJ , submitted

Newberg, H. ., Yanny, B., Grebel, E.K., Martinez-Delgado, D., Odenkirchen, M., Rix, H.-W., for the Sloan Digital Sky Survey Collaboration: 2005, ASP Conf. Ser., Vol. 317, ed. D. Clemens, R. Y. Shah, and T. Brainerd (San Francisco:ASP), 264

Nonino, M. et al.: 1999, A&AS 137, 51

Pier, J.R., Munn, J.A., Hindsley, R.B., Hennessy, G.S., Kent, S.M., Lupton, R.H., Ivezić, Z.: 2003, AJ 125, 1559

Richards, G.T., et al.: 2002, AJ 123, 2945

Rider, C.J., Tucker, D.L., Smith, J.A., Stoughton, C., Allam, S.S., Neilsen, E.H.: 2004, AJ 127, 2210

Rodgers, T.C., Canterna, R., Smith, J.A., Pierce, M.J., Tucker, D.L.: 2006, AJ , 132, 989

Sako, M., Romani, R., Frieman, J., et al.: 2005, Proceedings of the 22nd Texas Symposium on Relativistic Astrophysics, in press

Schechter, P.L., Mateo, M., Saha, A.: 1993, PASP 105, 1342

Sergey, G., Berman, E., Huang, C.-H., Kent, S., Newberg, H., Nicinski, T., Petravick, D., Stoughton, C.: 1996, in Astronomical Data Analysis Software and Systems V, ASP Conf. Ser., Vol. 101, ed. G. H. Jacoby & J. Barnes, (San Francisco:ASP), 248

Shostak, G.S., Allen, R.J.:1980, Two Dimensional Photometry, ed. P. Crane and K. Kjär (Published by ESO), p.169

Smith, J.A., Tucker, D.L., Kent, S., et al.: 2002, AJ 123, 2121

Smith, J.A., Tucker, D.L., Allam, S.S., Rodgers, C.T.: 2003, AJ 126, 2037

Stetson, P.B.: 1987, PASP 99, 191

Stoughton, C.: 1995, BAAS 187, 9101

Stoughton, C., et al.: 2002a, AJ , 123, 485 (EDR)

Stoughton, C., et al.: 2002b, Proceedings of the SPIE 4836, 339

Strauss, M.A. et al.: 2002, AJ 124, 1810

Tody, D.: 1986, Proceedings of the SPIE 627, 733

Tody, D.: 1993, in ASP Conf. Ser. 52, Astronomical Data Analysis Software and Systems II, ed. R.J. Hanisch, R.J.V. Brissenden, and J. Barnes (San Francisco: Astr. Soc. Pac.), p. 173

Valdes, F.G., Campusano, L.E., Velasquez, J.D., Stetson, P.B.: 1995, PASP 107, 1119

van der Hulst, J.M., Terlouw, J.P., Begeman, K.G., Zwister, W., Roelfsema: 1992, in ASP Conf. Ser. 25, Astronomical Data Analysis Software and Systems I, ed. D.M. Worrall, C. Biemesderfer, and J. Barnes (San Francisco: Astr. Soc. Pac.), p. 131

Warmels, R.H.: 1992, in ASP Conf. Ser. 25, Astronomical Data Analysis Software and Systems I, ed. D.M. Worrall, C. Biemesderfer, and J. Barnes (San Francisco: Astr. Soc. Pac.), p. 115

York, D.G., et al.: 2000, AJ 120, 1579